Distributionally robust multi-period humanitarian relief network design integrating facility location, supply inventory and allocation, and evacuation planning

Yunqiang Yin, Jie Wang, Feng Chu, Dujuan Wang

Distributionally robust multi-period humanitarian relief network design integrating facility location, supply inventory and allocation, and evacuation planning

Yunqiang Yin[a], Ji eW ang[a], Feng Chu[b] and Dujuan Wang[c]

[a]School of Management and Economics, University of Electronic Science and Technology of China, Chengdu, People's Republic of China; [b]IBISC, Univ Évry, University of Pairs-Saclay, Évry, France; [c]Business School, Sichuan University, Chengdu, People's Republic of China

Facility location, supply inventory and distribution, and evacuation planning are key operational functions in a humanitarian relief network, it is critical to integrate these three functions and sched-ule their activities jointly in a coordinated manner. Considering uncertain demands and evacuation rates of injured people, we develop a distributionally robust model for the multi-period humanitar-ian relief network design with multiple types of relief supplies. To solve the problem, we reformulate the proposed model into a mixed integer linear programme, and develop an enhanced branch-and-Benders-cut algorithm that incorporates some algorithm enhancements to solve the resulting model. Extensive numerical experiments show that: (i) the distributionally robust model provides more reliable and flexible solutions that perform the best when faced uncertainty over the deter-ministic and stochastic models; (ii) the algorithm enhancements are very effective to enhance the performance of the proposed algorithm, which can reduce the CPU time by up to 9.75% $\sim$ 41.64% on average; (iii) the integrated solution approach is more beneficial to solve the problem when compar-ing with a sequential solution approach; and (iv) some model parameters have significant impact on the solution structure, which can help decision maker set proper parameters to achieve the desired trade-off among the considered metrics.

1. Introduction

In recent years, more and more large-scale disaster events, no matter man-made or natural, cause mass casualties and enormous economic losses because of their great destructiveness and sudden attack. For example, in 2016, the persistent rainstorms in southern China triggered severe landslides and mudslides, leaving more than 73,000 people homeless and causing economic losses of 10 billion RMB (Zhang et al. 2019). In 2021, a 7.3 magnitude earthquake in Haiti affected about 800,000 people, and damaged or destroyed 138,000 houses. Thus, it is vital to devise an efficient humanitarian relief network to support humanitarian logistics in executing appropriate rescue operation during disaster (Das and Hanaoka 2014) so as to decrease the losses of life and property.

Most of the existing studies on disaster relief mainly focus on the location of distribution centre and relief supplies allocation problem considering efficiency and equity, and gave little thought to the transportation and allocation of injured people. However, an efficient emergency response network should be studied in an integrated way. The inventory and distribution of relief supplies is closely related to the number of injured people at the relief shelter. As mentioned in Li, Zhang, and Yu (2020), setting up temporary shelters as a point of connection between supply and demand can effectively improve relief efficiency, where the allocation of emergency relief distribution centres and allocation of relief supplies are considered on the supply side, and the allocation of injured people is considered on the demand side. With this in mind, to achieve optimal performance in a rescue operation, we integrate the aforementioned operations on both of the supply and demand sides and schedule their activities jointly in a coordinated manner.

However, this task is not easy to accomplish due to the distinct intrinsic characteristics of different disaster events, and the insufficient historical data. For example, in sudden disaster events such as earthquake and tsunamis, the demands of relief supplies in disaster areas are generally uncertain and vary with disaster

severity, and the minimum thresholds on the number of injured people that should be transferred to rescue shelters for timely treatment are also uncertain which highly depend on the severity of the affected areas. To deal with the demand uncertainty, we employ the distributionally robust optimisation (DRO) to characterise the uncertainty of the demands of relief supplies by so-called distributionally robust ambiguity set which only needs partial distribution information on uncertain parameters. This approach efficiently combines the advantages of robust optimisation (RO) and stochastic optimisation (SO) while avoiding their drawbacks, which can offer an attractive trade-off between the conservatism of robust optimisation and poor out-of-sample performance of stochastic optimisation (Rahimian, Bayraksan, and Homem-de 2019).

To sum up, we intend to design a distributionally robust multi-period humanitarian relief network with multiple types of relief supplies under uncertain demands and evacuation rates of injured people, which simultaneously determines the location of potential emergency relief distribution centres and temporarily rescue shelters, the inventory of relief supplies in the emergency relief distribution centres and rescue shelters, and the allocation of relief supplies from the emergency relief distribution centres to the rescue shelters and of the evacuation strategy of injured people from the affected areas to the rescue shelters over a finite planning horizon. The main contributions of this paper are as follows:

(i) We consider a novel distributionally robust multi-period humanitarian relief network optimisation model with multiple types of relief supplies under uncertain demands and evacuation rates of injured people with distributionally robust chance constraints. Unlike existing study on disaster relief, we simultaneously address the issues of facility location, supply inventory and allocation, and evacuation planning, and tackle the demand uncertainty by distributionally robust optimisation. The ambiguity set with limited distributional information about the support, mean, and upper bounds on the marginal dispersion and cross dispersion is introduced to characterise the distributions of demands, which is useful in capturing possible demand correlations across relief supplies and time periods. The distributionally robust chance constraints ensure that the demand of relief supplies in each time period is satisfied at a predefined level by taking their probability distributions within the ambiguity set into account. To the best of our knowledge, we are the first to study the integrated humanitarian relief network design problem of location-inventory-allocation and evacuation planning based on the DRO framework.

(ii) We derive an equivalent solvable mixed integer linear programme of the distributionally robust model by exploiting the structure of the ambiguity set, and develop a tailored exact branch-and-cut framework based on Benders decomposition (called branch-and-Benders-cut algorithm), that exploits the underlying problem structure, to solve the resulting model. We also introduce some non-trivial enhancements, including in–out Benders cut generation and initial cut generation, to enhance the proposed algorithm.

(iii) We perform computational study to discuss the computational efficiency of the developed algorithm, discuss the benefit of the distributionally robust model over the deterministic and stochastic models, and the benefit of our integrated solution approach over a sequential solution approach (injured people evacuation first, relief supplies allocation second), and observe the effects of changing specific model parameters to gain management implications.

The rest of this paper is organised as follows. In Section 2, we briefly review the related literature. In Section 3, we formally describe the problem under study, formulate the distributionally robust optimisation model, and reformulate it as a mixed-integer linear programme. In Section 4, we present an enhanced branch-and-Benders-cut algorithm to solve the resulting mixed-integer linear programme. In Section 5, we conduct extensive computational studies to assess the performance of the developed algorithm, and highlight the benefit of the distributionally robust model and the benefit of our integrated solution approach. Section 6 gives some conclusion of this work.

2. Literature review

The following literature review provides a brief summary of work that is most related to our study. The detailed comparison of the main problem characteristics and solution methods of the work are summarised in Table 1.

2.1. Optimisation problems for humanitarian relief network design

As one of the hotspots in the field of operations research management, the design of humanitarian relief network has attracted increasing attention from the operations research community. Many studies focus on facility

Table 1. Overview of humanitarian relief network models.

Reference	Optimisation criteria	Humanitarian network	Uncertainty factors	Period	Optimisation model	Solution method
Üster and Dalal (2017)	Fixed cost, flow cost, inbound cost	Location, allocation, capacity level, evacuation planning	–	Single	Multi-objective mixed integer programming model	Benders decomposition
Dalal and Üster (2018)	Fixed cost, flow cost	Location, allocation, evacuation planning	Location, demands	Single	Hybrid robust and stochastic model	Benders decomposition
Liu et al. (2019)	Construction costs, maintenance and purchase costs, transportation cost	Location, number of ambulances, demand assignment	Daily demands, maximum number of concurrent demands	Single	Distributionally robust model	Outer approximation algorithm
Li, Zhang, and Yu (2020)	Fixed cost, storage cost, transportation cost, penalty cost	Location, allocation, evacuation planning	Evacuee scales, travel times	Single	Hybrid robust and stochastic model	Customised progressive hedging algorithm
Zhang et al. (2021)	Fixed cost, transportation cost, penalty cost	Location, allocation, routing of vehicles	Travel times	Single	Distributionally robust model	Search algorithm with CPLEX
Li, Yu, and Zhang (2021)	Fixed cost, transportation cost, penalty cost, holding cost	Location, allocation, evacuation planning	Various scenarios of disasters	Single	Three-stage stochastic programming model	Benders decomposition
Dalal and Üster (2021)	Fixed cost, transportation cost, logistics cost	Location, allocation, evacuation planning	Disaster location, intensity, disaster duration time, evacuee compliance	Single	Robust optimisation model	Benders decomposition
Yang, Liu, and Yang (2021)	Fixed cost, transportation cost, holding cost, penalty cost	Location, allocation, capacity level	Demands	Multiple	Distributionally robust model	CPLEX
Shehadeh and Tucker (2022)	Fixed cost, transportation cost	Location, allocation, commodity preposition and delivery	Disasters type, demands, usable relief items, arc capacity, maximum order quantity	Single	Stochastic and distributionally robust model	Decomposition algorithm
Zhang et al. (2022)	Fixed cost, supplies delivered cost	Location, allocation	disaster severity, road condition and capacity, demand	Single	Multi-objective distributionally robust optimisation model	Revised multi-choice goal programming approach
Wang, Yang, and Yang (2023)	Fixed cost, acquisition cost, transportation cost, holding cost, penalty cost	Location, inventory, allocation	Supplies, demands, road link capacities	Single	Two-stage distributionally robust optimisation model	CPLEX
Yang et al. (2023)	Fixed cost, transportation cost, penalty cost	Location, allocation	Demands, travel times	Multiple	Distributionally robust optimisation	Benders decomposition
This paper	Fixed cost, storage cost, supply transportation cost, evacuation cost, penalty cost of non-evacuees	Location, inventory, allocation, evacuation planning	Demands, evacuation rates	Multiple	Distributionally robust optimisation model	Benders decomposition

location-allocation (including the location of rescue shelters and material storage facilities and the allocation of relief supplies) under uncertainty of the facility opening level (Yang et al. 2023), demands and travel times (Avishan et al. 2023 Caunhye et al. 2016; Li and Chung 2019), state of road network (Hu et al. 2019 Ni, Shu, and Song 2018) or disaster scenarios (Zhang et al. 2019), which aim to deliver relief supplies to affected areas timely and minimise total operation cost with the consideration of rescue efficiency and equity (Zhu et al. 2019). There are also studies that consider evacuation planning problems under uncertainty of the number of injured people (Mohammadi et al. 2020), disaster demands (Mete and Zabinsky 2010; Setiawan, Liu, and French 2019), or

evacuation rates and times (Caunhye and Nie 2018), and the goal of such kind of problems is more inclined to save more injured people or minimise the expected casualties or total rescue cost (Salmerón and Apte 2010).

Most of the aforementioned studies investigate location-allocation and evacuation planning problems separately, which may lead to significantly suboptimal solutions. This is mainly because the complexity of the integrated models and the difficulty of designing efficient algorithms for solving them. To the best of our knowledge, only a few studies consider integration of location-allocation and evacuation planning. Üster and Dalal (2017) focus on the strategic emergency preparedness network design integrating supply and demand sides, which involve a three-tier system with evacuation zone, shelter zone, and distribution centres (DCs). The objective is to determine the DC locations, shelter locations and capacity levels, and source-to-shelter and DC-to-shelter assignments and corresponding flows so as to simultaneously minimise the critical distance and the system cost. Dalal and Üster (2018) extend the model studied in Üster and Dalal (2017) by considering uncertain evacuating population and integrating the worst case and average costs in the objective under all the possible scenarios of evacuating population. Li, Zhang, and Yu (2020) explore scenario-based robust programming approach to model two main types of uncertainties by including stochastic scenarios for disaster severities and robust uncertainty sets for evacuee scales and transportation time. Dalal and Üster (2021) investigate a robust relief supply network comprising five entities, including evacuation sources, urban distribution centres, shelters, distribution centres, and centralised supply locations considering uncertainties in disaster location, intensity, duration, and evacuee compliance, where a combination of event and box uncertainty is used to characterise the uncertain parameters.

The above literature review shows that existing studies on integrated location-allocation and evacuation planning mainly focus on single period case and regard all the relief supplies as the same type. However, the rescue work after a disaster usually lasts several days, and multiple types of relief supplies are required for injured people. Therefore, it is vital to consider an overall response network design considering both supply (relief) and demand (evacuation) sides with multiple types of relief supplies in a multi-period setting. To this end, the main purpose of this paper is to provide a multi-period humanitarian relief network design integrating facility location, supply inventory and allocation, and evacuation planning that consider uncertain demands and evacuation rates of injured people, where the inventory in distribution centres and rescue shelters and multiple types of relief supplies are considered. Moreover, instead of using stochastic optimisation (SO) and robust optimisation (RO) methods, we introduce distributionally robust ambiguity set to characterise the uncertainty of the demands of relief supplies, and explore the DRO method to deal with the problem.

2.2. DRO for humanitarian relief network design

To cope with the uncertainty in humanitarian relief network design, most of the existing studies adopt SO methods (Dyen, Aras, and Gülay 2012; Li, Yu, and Zhang 2021), RO methods (Alizadeh et al. 2019; Ben-Tal et al. 2011) or a combination of SO and RO methods (Dalal and Üster 2018). However, SO suffers from imperfection that requires precise knowledge of the underlying true distributions of the uncertain parameters, which are generally difficult to obtain due to insufficiency of historical data in practice. RO does not fully utilise the distributional information on the uncertain parameters to enhance the solution quality, but the solution obtained from RO may be over-conservative since the worst-case realisation may only arise with a very small probability. Combining the advantages of both stochastic and robust optimisation while avoiding their disadvantage, DRO has received increasing attention in recent years (Luo et al. 2023; Yin et al. 2023). Several studies have employed DRO in humanitarian relief network design, where to our knowledge all the ambiguity sets to characterise the uncertain parameters are moment-based ambiguity sets that consist of all the distributions whose moments satisfy certain properties.

In the first-order moment ambiguity set setting, Yang, Liu, and Yang (2021) investigate multi-period dynamic distributionally robust pre-positioning of emergency supplies with distributionally robust chance constraints, and introduce bounded perturbation sets (box, box-ball and box-polyhedral) to characterise the uncertainty of demands. They develop a computationally tractable safe approximation of the chance constraints, and solve the resulting model directly using CPLEX. Shehadeh and Tucker (2022) propose a distributionally robust location-inventory-allocation model, where a mean-support ambiguity set is introduced to characterise the uncertainty of disaster level, affected areas' locations, and demands of relief supplies. They develop a simple decomposition algorithm to solve the equivalent reformulation. Zhang et al. (2022) develop a multi-objective DRO model for a sustainable last mile relief network problem that simultaneously maximises the equitable distribution of relief supplies and minimises the transportation time and operation cost, where a first-order moment ambiguity set incorporating the support,

mean and mean absolute deviations is used to characterise the uncertain parameters including disaster situation, transportation time, freight, road capacity, and demand. Wang, Yang, and Yang (2023) put forward a two-stage distributionally robust location-inventory-allocation model with multiple types of relief supplies based on the worst-case mean-conditional value-at-risk criterion, and introduce two types of first-order moment ambiguity sets (box and polyhedral) incorporating the support, mean, and mean absolute deviations to characterise the uncertainty of relief supplies, demands, and road link capacities. They show that the model under the two types of ambiguity sets can be reformulated as mixed integer linear programmes, which are directly solved using CPLEX. Yang et al. (2023) present a DRO model for the multi-period location-allocation problem with multiple resources and capacity levels under the uncertainty of emergency demands and resource fulfilment times, where the first-order moment ambiguity sets incorporating the support, mean, and mean absolute deviations are used to characterise the uncertain parameters, and developed a branch-and-Benders-cut algorithm to solve the resulting reformulation. The work on second-order moment ambiguity set is relatively few. To the best of our knowledge, only Liu et al. (2019) and Zhang et al. (2021) follow this line. Specifically, Liu et al. (2019) study the DRO of an emergency medical service station location with distributionally robust joint chance constraints, where an ambiguity set with second-order moment information is used to characterise the uncertainty of demands. They reformulate the proposed model into a parametric second-order cone programme (SOCP), and develop an outer approximation algorithm to solve a special case of the proposed model. Zhang et al. (2021) develop a DRO model for the location-allocation problem with distributionally robust chance constants under the uncertainty of travel times characterised by a second-order moment ambiguity set, and reformulate the DRO model into a SOCP.

The above literature review illustrates that most studies in humanitarian relief network design focus on first-order moment ambiguity sets incorporating the support, mean, and mean absolute deviations to characterise uncertain parameters. Our study follows this line. However, compared with the aforementioned studies, we integrate the cross-dispersion into the ambiguity set to capture both the demand correlations across relief supplies and time periods. Moreover, considering that the reliability and confidence level of the model should be considered in the design of humanitarian relief network, as in Yang, Liu, and Yang (2021) and Zhang et al. (2021), we impose distributionally robust chance constraints to ensure that the demand of relief supplies in each time period is satisfied at a predefined level by taking their probability distributions within the ambiguity set into account. Finally, compared with most studies which directly solve the reformulations using commercial software, we develop an enhanced branch-and-Benders-cut algorithm to deal with the proposed integrated model. Although a similar solution algorithm has already been developed in Yang et al. (2023), the contribution of this paper is to extend this solution algorithm in order to optimally solve the resulting reformulation of the problem for large-scale instances.

To sum, our study endeavours to employ a DRO approach to address the integrated location-inventory-allocation and evacuation planning in the design of multi-period humanitarian relief network, and evaluate the benefit of considering distribution robustness and the benefit of simultaneously optimising facility location, supply inventory and allocation, and evacuation planning.

3. Problem description and model formulation

In this section, we briefly describe the humanitarian relief network model we consider, and formulate the distributionally robust optimisation model, and show how to transform it into an equivalently deterministic model. The main notation used in this paper is listed in Table 2.

3.1. Problem description

As shown in Figure 1, we consider a multi-period humanitarian relief network, consisting of emergency relief distribution centres, rescue shelters, and affected areas. When a disaster occurs, humanitarian relief organisations need to transport relief supplies from emergency relief distribution centres to rescue shelters timely, while the injured people should be evacuated from affected areas to rescue shelters for immediate treatment. In our humanitarian relief network design, the operation of disaster relief activities is divided into two phases, i.e. pre-disaster phase and emergency response phase. In pre-disaster phase, some emergency relief distribution centres and rescue shelters are chosen from a set of potential locations to open at a capacity level. On the other hand, in emergency response phase, injured people are transferred to the opened rescue shelters for immediate treatment, and different types of relief supplies (like water, medicine, food, tent and so on) are transported to these rescue shelters to meet their demand.

The distributionally robust humanitarian network design integrating facility location, resource inventory and allocation, and evacuation planning, denoted as DRHND-FLRIAEP, considers the setting up a subset of

Table 2. Notation table.

Sets
M: the set of candidate emergency relief distribution centres with index i.
E: the set of existing rescue shelters with index j.
N: the set of candidate relief stations with index j.
G: the set of affected areas with index k.
R: the set of relief supplies with index r.
Parameters
f_{it}^{d}: the fixed open cost of emergency relief distribution centre i during time period t.
f_{jt}^{r}: the fixed open cost of new rescue shelter j during time period t.
Q_{ir}^{d}: the maximum inventory capacity for relief supply r at emergency relief distribution centre i.
Q_{j}^{ri}: the maximum inventory capacity for relief supply r at rescue shelter j.
Q_{j}^{rh}: the maximum inventory capacity for injured people at rescue shelter j.
ϑ_{irt}: the amount of relief supplies r supplied by the suppliers to emergency relief distribution centre i during time period t.
c_{irt}^{s}: the unit storage cost of relief supplies r at emergency relief distribution centre i during time period t.
c_{ijt}^{t}: the unit transportation cost of relief supplies between emergency relief distribution centre i and rescue shelter j during time period t.
n_{kt}: the new injured people at affected area k that need to be transferred during time period t.
Len_{jk}: the distance between affected area k and rescue shelter j.
Q_{jk}^{c}: the capacity of the arc between affected area k and rescue shelter j.
c_{jkt}^{e}: the evacuation cost for transferring one person from affected area k to rescue shelter j during time period t.
ϖ: the maximum evacuation distance.
τ_{kt}: the unit penalty cost of non-evacuees at affected area k during time period t.
$\tilde{\kappa}_{rt}$: the unit demand of injuries for relief supplies r during time period t.
$\tilde{\alpha}_{kt}$: the evacuation rate of injured people at affected area k during time period t.
μ_{rt} : the estimated mean value of unit demand $\tilde{\kappa}_{rt}$.
σ_{rt} : the upper bound on the mean-absolute deviation of unit demand $\tilde{\kappa}_{rt}$.
ξ_{t} : the upper bound on the mean-absolute deviation of the aggregated random demand $\sum_{l=1}^{t}\sum_{r\in R}\tilde{\kappa}_{rt}$.
γ_{rt}: the risk level.
Variables
x_{it} : 1 if emergency relief distribution centre i is opened during time period t, and 0 otherwise.
y_{jt} : 1 if temporary rescue shelter j is opened during time period t, and 0 otherwise.
z_{jkt} : 1 if affected area k is allocated to rescue shelter j during time period t, and 0 otherwise.
h_{jkt}: the percentage of injured people at affected area k that are allocated to rescue shelter j during time period t.
Δ_{kt} : the percentage of injured people at affected area k who are not evacuated during time period t.
q_{ijrt} : the amount of relief supplies r delivered from emergency relief distribution centre i to rescue shelter j during time period t.
δ_{irt} : the amount of relief supplies r stored at emergency relief distribution centre i during time period t with initial inventory of relief supplies $\delta_{ir0} = Q_{ir}^{d}$.

potential emergency relief distribution centres and a subset of temporarily rescue shelters, and the designing of relief supplies delivery scheme from the emergency relief distribution centres to the rescue shelters and of the evacuation strategy of injured people from the affected areas to the rescue shelters over a finite planning horizon T.

Specifically, DRHND-FLRIAEP is defined on a graph $G = (V, A)$, where $V = M \cup N \cup E \cup G$ is the node set, and $A = \{(i,j) : i \in M, j \in N \cup E\} \cup \{(j,k) : j \in N \cup E, k \in G\}$ is the arc set. Here, M is the set of candidate emergency relief distribution centres, E is the set of existing rescue shelters (such as clinics, pharmacies, and medical services), N is the set of candidate relief stations (such as temporarily built-in parks, schools, and other places), and G is the set of affected areas.

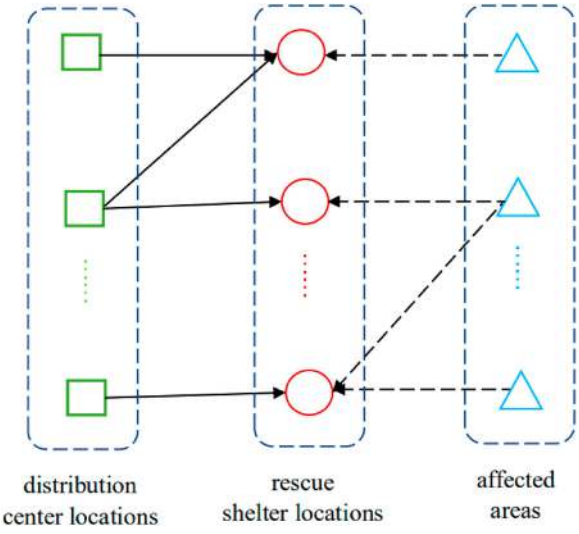

Figure 1. Emergency rescue network.

Opening emergency relief distribution centre $i \in M$ and rescue shelter $j \in E$ during time period t incurs fixed costs f_{it}^{d} and f_{jt}^{r}, respectively. Each emergency relief distribution centre $i \in M$ stores a set of different kinds of relief supplies R, and has a maximum inventory capacity Q_{ir}^{d} for relief supply $r \in R$. Each rescue shelter $j \in N \cup E$ has a maximum inventory capacity Q_{j}^{ri} for relief supplies and a maximum holding capacity Q_{j}^{rh} for injured people.

During the rescue period, suppliers continuously provide enough relief supplies to the emergency relief distribution centres, and the amount of relief supplies r supplied from the suppliers to relief distribution centre $i \in M$ during time period t is ϑ_{irt}. In resource allocation stage, the decision-maker needs to determine the amount of relief supplies stored in the distribution centres, and the amount of relief supplies transferred from the distribution centres to rescue shelters. Denote by c_{irt}^{s} and c_{ijt}^{t} the unit storage cost of relief supplies r at emergency relief distribution centre i, and the unit transportation cost of relief supplies between emergency relief distribution centre i and rescue shelter j during time period t, respectively.

In casualty evacuation stage, the injured people need to be transferred to rescue shelters for timely treatment. In each time period t, there are n_{kt} new injured people at affected area k that need to be transferred to rescue shelters for treatment. The distance between affected area k and rescue shelter j is Len_{jk}, the capacity of the arc

between affected area k and rescue shelter j is Q^c_{jk}, and the evacuation cost for transferring one person from affected area k to rescue shelter j during time period t is c^e_{jkt}. In order to get timely treatment, we assume that the injured people at an affected area can only be transferred to rescue shelters whose distance from the affected area does not exceed a threshold ϖ, which also reflects the equity for transferring the injured people. Due to the limited rescue capacity, some injured people may not be timely transferred to rescue shelters during a time period, who will be transferred in the subsequent time period, and let τ_{kt} be the penalty cost per person at affected area k who has not been evacuated during time period t.

Due to the complexity of disaster environment, we could not accurately capture the severity of the injuries. Therefore, we assume that the demand per person for relief supply r during time period t, $\tilde{\kappa}_{rt}$ is uncertain, which usually cannot be accurately estimated. For example, it is hard to predict the blood and medications types required due to individual-level differences. However, we assume that some partial information on $\tilde{\kappa}_{rt}$, such as the lower and upper bounds of demands and the expected demands, can be obtained through historical data, and that the distribution is ambiguous and varies within an ambiguity set that is characterised by the available partial information on the support, mean, dispersion bounds, and partial cross moment information of the distribution of $\tilde{\boldsymbol{\kappa}} = (\tilde{\kappa}_{rt})_{r\in R, t\in\{1,2,\cdots,T\}}$. Specifically, referring to Wang, Chen, and Liu (2020), we consider the following ambiguity set:

$$\mathbb{F}_\kappa = \left\{ \mathbb{P} \left| \begin{array}{ll} \mathbb{E}_{\mathbb{P}}(\tilde{\kappa}_{rt}) = \mu_{rt} & \forall r \in R, \\ & t \in \{1,2,\cdots T\} \\ \mathbb{E}_{\mathbb{P}}(|\tilde{\kappa}_{rt} - \mu_{rt}|) \le \sigma_{rt} & \forall r \in R, \\ & t \in \{1,2,\cdots T\} \\ \mathbb{E}_{\mathbb{P}}\left(\left|\sum_{l=1}^{t} 1'(\tilde{\boldsymbol{\kappa}}^l - \boldsymbol{\mu}^l)\right|\right) \le \xi_t & \forall t \in \\ & \{1,2,\cdots T\} \\ \mathbb{P}(\in Q) = 1 & \end{array} \right. \right\} \quad (1)$$

where the support set Q of $\tilde{\boldsymbol{\kappa}}$ is given as:

$$Q = \{\tilde{\boldsymbol{\kappa}} | \tilde{\kappa}_{rt} \in [l_{rt}, e_{rt}], \forall r \in R, t \in \{1,2,\cdots,T\}\} \quad (2)$$

Here, the first constraint set of ambiguity set $_\kappa$ captures the expected demand per person for relief supply r during time period t; the second constraint set represents the marginal dispersion of $\tilde{\kappa}_{rt}$ around its mean μ_{rt}; the third constraint set uses the cross-dispersion that provides the correlation information of the random variables $\tilde{\boldsymbol{\kappa}}^l$ in time period l by imposing the upper bound ξ_t on the mean-absolute deviation of the aggregated random demand $\sum_{l=1}^{t}\sum_{r\in R}\tilde{\kappa}_{rt}$, which can capture both the demand correlations across relief supplies and time periods; and the last constraint set defines the support set of $\tilde{\boldsymbol{\kappa}}$. The parameters σ_{rt} and ξ_t can quantify the discrepancy, which reflects the decision makers' belief regarding the nominal probability distribution of $\tilde{\boldsymbol{\kappa}}$.

Moreover, as mentioned in Dalal and Üster (2021), it is crucial to impose a minimum threshold on the number of injured people that should be transferred to rescue shelters for timely treatment, which affects the willingness of the people in disaster areas to be evacuated to a certain extent. However, this threshold highly depends on the severity of each affected area, which is usually uncertain. Referring to Dalal and Üster (2021), we assume that the evacuation rate of injured people at affected area k during time period t, $\tilde{\alpha}_{kt}$ lies in a symmetric interval around their nominal values $\bar{\alpha}_{kt} \in [0,1]$, i.e.

$$\tilde{\alpha}_{kt} \in [\,\bar{\alpha}_{kt}(1-\epsilon_1),\ \bar{\alpha}_{kt}(1+\epsilon_1)] \quad (3)$$

where $\epsilon_1 \in [0,1]$ is a predefined parameter.

The objective is to determine the set of emergency relief distribution centres and temporary rescue shelters to open, and the strategies of storing relief supplies at emergency relief distribution centres and delivering relief supplies from the emergency relief distribution centres to the rescue shelters and transferring the injured people from the affected areas to the rescue shelters, so as to minimise the total cost consisting of the fixed cost of opening the emergency relief distribution centres and temporary rescue shelters, the storage and transportation costs of relief supplies, the evacuation cost of injured people, and the penalty cost of non-evacuees.

3.2. Model formulation

We formulate the distributionally robust model for the problem under consideration, denoted as *DRM*, as follows:

$$\begin{aligned} \min & \sum_{t=1}^{T}\sum_{i\in M} f^d_{it}x_{it} + \sum_{t=1}^{T}\sum_{j\in N} f^r_{jt}y_{jt} \\ & + \sum_{t=1}^{T}\sum_{i\in M}\sum_{j\in N\cup E}\sum_{r\in R} c^t_{ijt}q_{ijrt} \\ & + \sum_{t=1}^{T}\sum_{i\in M}\sum_{r\in R} c^s_{irt}\delta_{irt} \\ & + \sum_{t=1}^{T}\sum_{k\in G}\sum_{j\in N\cup E} Len_{jk}c^e_{jkt}h_{jkt}n_{kt} + \sum_{t=1}^{T}\sum_{k\in G}\tau_{kt}\Delta_{kt}n_{kt} \end{aligned}$$

Subject to

$$x_{it} \ge x_{i,t-1} \quad \forall i \in M, t \in \{2,3,\cdots,T\} \quad (4)$$

$$y_{jt} \ge y_{j,t-1} \quad \forall j \in N, t \in \{2,3\cdots,T\} \quad (5)$$

$$\sum_{i\in M} q_{ijrt} \le y_{jt}Q^{ri}_j \quad \forall j \in N, r \in R, t \in \{1,2,\cdots,T\} \quad (6)$$

$$\sum_{i\in M} q_{ijrt} \le Q_j^{ri} \quad \forall j \in E, r \in R, t \in \{1,2,\cdots,T\} \tag{7}$$

$$\delta_{irt} \le x_{it} Q_{ir}^{d} \quad \forall i \in M, r \in R, t \in \{1,2,\cdots,T\} \tag{8}$$

$$\sum_{j\in N\cup E} q_{ijrt} \le x_{it} Q_{ir}^{d} \quad \forall i \in M, r \in R, t \in \{1,2,\cdots,T\} \tag{9}$$

$$\delta_{irt} = \delta_{ir,t-1} + \vartheta_{irt} - \sum_{j\in N\cup E} q_{ijrt} \quad \forall i \in M, r \in R, t \in \{1,2,\cdots,T\} \tag{10}$$

$$\sum_{j\in N\cup E} h_{jkt} + \Delta_{kt} = 1 \quad \forall k \in G, t \in \{1,2,\cdots,T\} \tag{11}$$

$$\sum_{s=1}^{t}\sum_{k\in G} h_{jks} n_{ks} \le y_{jt} Q_j^{rh} \quad \forall j \in N, t \in \{1,2,\cdots,T\} \tag{12}$$

$$\sum_{s=1}^{t}\sum_{k\in G} h_{jks} n_{ks} \le Q_j^{rh} \quad \forall j \in E, t \in \{1,2,\cdots,T\} \tag{13}$$

$$h_{jkt} n_{kt} \le z_{jkt} Q_{jk}^{c} \quad \forall k \in G, j \in N\cup E, t \in \{1,2,\cdots,T\} \tag{14}$$

$$\sum_{j\in N\cup E} h_{jkt} \ge \min\{1, \tilde{\alpha}_{kt}\} \quad \forall k \in G, t \in \{1,2,\cdots,T\},$$

$$\tilde{\alpha}_{kt} \in [\,\bar{\alpha}_{kt}(1-\epsilon_1),\ \bar{\alpha}_{kt}(1+\epsilon_1)] \tag{15}$$

$$Len_{jk} z_{jkt} \le \varpi \quad \forall k \in G, j \in N\cup E, t \in \{1,2,\cdots,T\} \tag{16}$$

$$z_{jkt} \le y_{jt} \quad \forall k \in G, j \in N, t \in \{1,2,\cdots,T\} \tag{17}$$

$$\inf_{\in_\kappa} \left\{ \sum_{i\in M}\sum_{j\in N\cup E} q_{ijrt} \ge \tilde{\kappa}_{rt} \sum_{j\in N\cup E}\sum_{k\in G} h_{jkt} n_{kt} \right\} \ge 1-\gamma_{rt} \quad \forall r \in R, t \in \{1,2,\cdots,T\} \tag{18}$$

$$x_{it}, y_{jt}, z_{jkt} \in \{0,1\}, q_{ijrt}, h_{jkt}, \delta_{irt}, \Delta_{kt} \ge 0, \quad \forall i \in M, j \in N\cup E, r \in R, k \in G, t \in \{1,2,\cdots,T\} \tag{19}$$

The objective function is to minimise the total cost. Constraints (4) (resp., (5)) guarantee that an opened emergency relief distribution centre (resp., rescue shelter) in a time period remains open in the subsequent time periods. Constraints (6) and (7) together state that relief supplies can only be delivered to the usable rescue shelters, and that the amount of relief supplies delivered to a rescue shelter should not exceed its maximum inventory capacity. Constraints (8) and (9) indicate that both the amount of relief supplies stored at an opened emergency relief distribution centre and the amount of relief supplies delivered from the opened emergency relief distribution centre in each time period cannot exceed its maximum inventory capacity, respectively. Constraints (10) give the distribution and storage balance equation at each emergency relief distribution centre in each time period. Constraints (11) give the evacuation flow in each affected area. Constraints (12) and (13) together ensure that injured people can only be transferred to the usable rescue shelters, and that the amount of relief supplies delivered to a rescue shelter should not exceed its maximum galleryful. Constraints (14) guarantee that the number of injured people transferred from an affected area to a rescue shelter should not exceed the capacity of the corresponding arc. Constraints (15) indicate that the transfer proportion of injured people at each affected area in each time period should not be less than the minimum threshold. Constraints (16) ensure that the injured people at an affected area can only be transferred to the usable rescue shelters whose distance from the affected area does not exceed a threshold ϖ. Constraints (17) indicate that the injured people can only be evacuated to the opened rescue shelters. Constraints (18) give the distributionally robust chance constraints, which ensure that the amount of relief supplies delivered to the rescue shelters in each time period being no less than the realised demand is satisfied with a probability of at least $1-\gamma_{rt}$ regarding all the distributions $\mathbb{P}$ in the ambiguity set $_\kappa$. Constraints (19) define the decision variables.

Remark 3.1: Although we assume that $\tilde{\alpha}_{kt} \in [\,\bar{\alpha}_{kt}(1-\epsilon_1),\ \bar{\alpha}_{kt}(1+\epsilon_1)]$, our model and solution method are easily adapted to the case where the uncertain parameters $\tilde{\alpha}_{kt}$ are characterised by ambiguity set as that for $\tilde{\kappa}_{rt}$. For example, in the *DRM* we can replace Constraints (15) with distributionally robust chance constraints as Constraints (18).

3.3. Tractable reformulation

In this section, we demonstrate how to reformulate the *DRM* as a solvable mixed integer linear programme by transforming the Constraints (15) and (18) into tractable reformulations.

In regard to Constraints (15), the following result is valid.

Proposition 3.2: *Constraints* (15) *are equivalent to the following constraints:*

$$\sum_{j\in N\cup E} h_{jkt} \ge \min\{1, \bar{\alpha}_{kt}(1+\epsilon_1)\} \quad \forall k \in G, t \in \{1,2,\cdots,T\} \tag{20}$$

Proof: Since $\tilde{\alpha}_{kt}$ is in the right-hand side of constraints (15), there exist an optimal solution such that $\tilde{\alpha}_{kt}$ takes its maximum value $\bar{\alpha}_{kt}(1+\epsilon_1)$, as required. ■

To transform the distributionally robust chance constraints (18) into tractable reformulations. Let us first introduce the following auxiliary lemma.

Lemma 3.3: *(Yang et al. 2023) Constraints*

$$\sum_{j\in J} a_j\xi_j \geq b, \quad \forall \xi_j \in [\underline{\xi}_j, \bar{\xi}_j] \tag{21}$$

are equivalent to the following constraint

$$\sum_{j\in J} a_j\xi_j^* - \varrho_j|a_j| \geq b \tag{22}$$

where $\xi_j^* = \frac{\underline{\xi}_j+\bar{\xi}_j}{2}$ and $\varrho_j = \frac{\bar{\xi}_j-\underline{\xi}_j}{2}$.

Let $\kappa_{rt}^* = \frac{l_{rt}+e_{rt}}{2}$ and $\zeta_{rt} = \frac{e_{rt}-l_{rt}}{2}$, $\tilde{\kappa}_{rt} \in [l_{rt}, e_{rt}]$. We have the following result.

Proposition 3.4: *Given the ambiguity set $_\kappa$, the evacuation planning $(h_{jkt})_{k\in G,j\in N\cup E,t\in\{1,2,\cdots T\}}$ and the rescue resource allocation strategy $(q_{ijrt})_{i\in M,j\in N\cup E,r\in R,t\in\{1,2,\cdots T\}}$, the distributionally robust chance constraints* (18) *are equivalent to the following constraint system:*

$$\beta\gamma_{rt} + \mu_{rt}\eta_{rt} + \sigma_{rt}(\phi_{rt}^+ + \phi_{rt}^-) + \xi_t(\Gamma_t^+ + \Gamma_t^-) + \theta \leq 0 \tag{23}$$

$$\begin{aligned}
&\kappa_{rt}^*\left(\eta_{rt} + \phi_{rt}^+ - \phi_{rt}^- + \Gamma_t^+ - \Gamma_t^- - \sum_{j\in N\cup E}\sum_{k\in G} h_{jkt}n_{kt}\right) \\
&\quad - \zeta_{rt}A_{rt} + \sum_{t'=1}^{t}\sum_{\boldsymbol{r}'\in R,(r',t')\neq(r,t)} (\kappa_{r't'}^*(\Gamma_t^+ - \Gamma_t^-) - \zeta_{r't'}C_t) \\
&\quad - \mu_{rt}(\phi_{rt}^+ - \phi_{rt}^-) + \sum_{t'=1}^{t}\sum_{\boldsymbol{r}'\in R}\mu_{r't'}(\Gamma_t^+ - \Gamma_t^-) + \theta \\
&\geq -\sum_{i\in M}\sum_{j\in N\cup E} q_{ijrt} - \beta
\end{aligned} \tag{24}$$

$$\begin{aligned}
&\kappa_{rt}^*(\eta_{rt} + \phi_{rt}^+ - \phi_{rt}^- + \Gamma_t^+ - \Gamma_t^-) - \zeta_{rt}B_{rt} \\
&\quad + \sum_{t'=1}^{t}\sum_{\boldsymbol{r}'\in R,(r',t')\neq(r,t)} (\kappa_{r't'}^*(\Gamma_t^+ - \Gamma_t^-) - \zeta_{r't'}C_t) \\
&\quad - \mu_{rt}(\phi_{rt}^+ - \phi_{rt}^-)\sum_{t'=1}^{t}\sum_{\boldsymbol{r}'\in R}\mu_{r't'}(\Gamma_t^+ - \Gamma_t^-) + \theta \geq 0
\end{aligned} \tag{25}$$

$$\eta_{rt} + \phi_{rt}^+ - \phi_{rt}^- + \Gamma_t^+ - \Gamma_t^- - \sum_{j\in N\cup E}\sum_{k\in G} h_{jkt}n_{kt} \geq -A_{rt} \tag{26}$$

$$\eta_{rt} + \phi_{rt}^+ - \phi_{rt}^- + \Gamma_t^+ - \Gamma_t^- - \sum_{j\in N\cup E}\sum_{k\in G} h_{jkt}n_{kt} \leq A_{rt} \tag{27}$$

$$\eta_{rt} + \phi_{rt}^+ - \phi_{rt}^- + \Gamma_t^+ - \Gamma_t^- \geq -B_{rt} \tag{28}$$

$$\eta_{rt} + \phi_{rt}^+ - \phi_{rt}^- + \Gamma_t^+ - \Gamma_t^- \leq B_{rt} \tag{29}$$

$$\Gamma_t^+ - \Gamma_t^- \geq -C_t \tag{30}$$

$$\Gamma_t^+ - \Gamma_t^- \leq C_t \tag{31}$$

$$\phi_{rt}^+, \phi_{rt}^-, \Gamma_t^+, \Gamma_t^-, A_{rt}, B_{rt}, C_t \geq 0 \tag{32}$$

Proof: The details of the proof are presented in Appendix 1. ■

Thus, according to the above tractable reformulation, we have the following result.

Theorem 3.5: *Given the ambiguity set $_\kappa$, the DRM is equivalent to the following deterministic mixed integer linear programme, denoted as D-MILP:*

$$\begin{aligned}
\min &\sum_{t=1}^{T}\sum_{i\in M} f_{it}^d x_{it} + \sum_{t=1}^{T}\sum_{j\in N} f_{jt}^r y_{jt} \\
&+ \sum_{t=1}^{T}\sum_{i\in M}\sum_{j\in N\cup E}\sum_{r\in R} c_{ijt}^t q_{ijrt} \\
&+ \sum_{t=1}^{T}\sum_{i\in M}\sum_{r\in R} c_{irt}^s \delta_{irt} \\
&+ \sum_{t=1}^{T}\sum_{k\in G}\sum_{j\in N\cup E} Len_{jk}c_{jkt}^e h_{jkt}n_{kt} \\
&+ \tau\sum_{t=1}^{T}\sum_{k\in G}\Delta_{kt}n_{kt}
\end{aligned}$$

s.t.

Constraints (4)–(14), (16)–(17), (19)–(20), (23)–(32)

4. Solution method

In this section, we develop a branch-and-Benders-cut algorithm based on Benders decomposition to optimally solve the *D-MILP*. Benders decomposition is well suited for humanitarian relief network design problems (Bayram and Yaman 2018; Caunhye and Nie 2018; Dalal and Üster 2018; Dalal and Üster 2021; Li, Yu, and Zhang 2021; Yang et al. 2023), as the problems can be decomposed into linear subproblems by fixing the integer variables for the location of relief distribution centres and rescue shelters. For our study, in Benders decomposition, the *D-MILP* is decomposed into a master problem (*MP*) and a Benders subproblem (*SP*). The *MP* mainly contains the opening variables of distribution centres $\boldsymbol{x} = (x_{it})_{i\in M,t\in\{1,2,\cdots,T\}}$ and new rescue

shelters $\boldsymbol{y} = (y_{jt})_{j\in N, t\in\{1,2,\cdots,T\}}$, the evacuation variables $\boldsymbol{z} = (z_{jkt})_{k\in G, j\in N\cup E, t\in\{1,2,\cdots,T\}}$, and an artificial variable representing a lower bound on the total cost of the subproblem. The subproblem contains the remaining continuous variables. The resulting model is solved by a Benders decomposition algorithm.

In the following subsections we introduce the Benders decomposition for our problem, show how to improve the basic Benders decomposition algorithm, and present the overall branch-and-Benders-cut algorithm.

4.1. Benders decomposition

4.1.1. Benders reformulation

By fixing the binary variables $\bar{\boldsymbol{x}} = (\bar{x}_{it})_{i\in M, t\in\{1,2,\cdots,T\}}$, $\bar{\boldsymbol{y}} = (\bar{y}_{jt})_{j\in N, t\in\{1,2,\cdots,T\}}$ and $\bar{\boldsymbol{z}} = (\bar{z}_{jkt})_{k\in G, j\in N\cup E, t\in\{1,2,\cdots,T\}}$, we can derive the following Benders subproblem, denoted as $SP\ (\bar{\boldsymbol{x}}, \bar{\boldsymbol{y}}, \bar{\boldsymbol{z}})$, in the space of other continuous variables:

$$\begin{aligned}\min \sum_{t=1}^{T}\sum_{i\in M}\sum_{j\in N\cup E}\sum_{r\in R} c^t_{ijt} q_{ijrt} + \sum_{t=1}^{T}\sum_{i\in M}\sum_{r\in R} c^s_{irt}\delta_{irt} \\ + \sum_{t=1}^{T}\sum_{k\in G}\sum_{j\in N\cup E} Len_{jk} c^e_{jkt} h_{jkt} n_{kt} \\ + \sum_{t=1}^{T}\sum_{k\in G} \tau_{kt}\Delta_{kt} n_{kt}\end{aligned}$$

s.t.

Constraints (20), (23) − (32)

$$\sum_{j\in N\cup E} q_{ijrt} \le \bar{x}_{it} Q^d_{ir} \quad \forall i\in M, r\in R, t\in\{1,2,\cdots,T\} \tag{33}$$

$$\sum_{i\in M} q_{ijrt} \le \bar{y}_{jt} Q^{ri}_j \quad \forall j\in N, r\in R, t\in\{1,2,\cdots,T\} \tag{34}$$

$$\sum_{i\in M} q_{ijrt} \le Q^{ri}_j \quad \forall j\in E, r\in R, t\in\{1,2,\cdots,T\} \tag{35}$$

$$\delta_{irt} \le \bar{x}_{it} Q^d_{ir} \quad \forall i\in M, r\in R, t\in\{1,2,\cdots,T\} \tag{36}$$

$$\sum_{j\in N\cup E} h_{jkt} + \Delta_{kt} = 1 \quad \forall k\in G, t\in\{1,2,\cdots T\} \tag{37}$$

$$\delta_{irt} = \delta_{ir,t-1} + \vartheta_{irt} - \sum_{j\in N\cup E} q_{ijrt} \quad \forall i\in M, r\in R, \\ t\in\{1,2,\cdots,T\} \tag{38}$$

$$\sum_{s=1}^{t}\sum_{k\in G} h_{jks} n_{ks} \le \bar{y}_{jt} Q^{rh}_j \quad \forall j\in N, t\in\{1,2,\cdots,T\} \tag{39}$$

$$\sum_{s=1}^{t}\sum_{k\in G} h_{jks} n_{ks} \le Q^{rh}_j \quad \forall j\in E, t\in\{1,2,\cdots,T\} \tag{40}$$

$$h_{jkt} n_{kt} \le \bar{z}_{jkt} Q^c_{jk} \quad \forall k\in G, j\in N\cup E, t\in\{1,2,\cdots,T\} \tag{41}$$

$$q_{ijrt}, \delta_{irt}, \Delta_{kt}, \phi^+_{rt}, \phi^-_{rt}, \Gamma^+_t, \Gamma^-_t, A_{rt}, B_{rt}, C_t \ge 0 \tag{42}$$

Let $\boldsymbol{p}, \boldsymbol{l}^+, \boldsymbol{l}^-, \boldsymbol{f}, \boldsymbol{e}, \boldsymbol{g}, \boldsymbol{v}^+, \boldsymbol{v}^-, \boldsymbol{s}, \boldsymbol{\rho}, \boldsymbol{u}^+, \boldsymbol{u}^-, \boldsymbol{o}^+, \boldsymbol{o}^-, \boldsymbol{w}^+, \boldsymbol{w}^-, \boldsymbol{\Lambda}, \boldsymbol{\Upsilon}^+, \boldsymbol{\Upsilon}^-$ be the dual variables associated with constraints (33)–(41), (20) and (23)–(31), respectively. Given $\kappa^*_{rt} = \frac{l_{rt}+e_{rt}}{2}$ and $\zeta_{rt} = \frac{e_{rt}-l_{rt}}{2}$, by the dual theory, the dual of $SP\ (\bar{\mathbf{x}}, \bar{\mathbf{y}}, \bar{\mathbf{z}})$, denoted as $DSP\ (\bar{\mathbf{x}}, \bar{\mathbf{y}}, \bar{\mathbf{z}})$, is formulated as follows:

$$\begin{aligned} max\ & -\sum_{t=1}^{T}\sum_{i\in M}\sum_{r\in R} \bar{x}_{it} Q^d_{ir}(p_{irt} + f_{irt}) \\ & - \sum_{t=1}^{T}\sum_{j\in N}\sum_{r\in R} \bar{y}_{jt} Q^{ri}_j l^+_{jrt} - \sum_{t=1}^{T}\sum_{j\in E}\sum_{r\in R} Q^{ri}_j l^-_{jrt} \\ & + \sum_{t=1}^{T}\sum_{k\in G} e_{kt} + \sum_{t=1}^{T}\sum_{i\in M}\sum_{r\in R} \vartheta_{irt} g_{irt} \\ & - \sum_{t=1}^{T}\sum_{j\in N} \bar{y}_{jt} Q^{rh}_j v^+_{jt} - \sum_{t=1}^{T}\sum_{j\in E} Q^{rh}_j v^-_{jt} \\ & - \sum_{t=1}^{T}\sum_{j\in N\cup E}\sum_{k\in G} \bar{z}_{jkt} Q^c_{jk} s_{jkt} \\ & + \sum_{t=1}^{T}\sum_{k\in G} min\{1, \bar{\alpha}_{kt}(1+\epsilon_1)\}\rho_{kt} \end{aligned}$$

s.t.

$$-p_{irt} - l^+_{jrt} + g_{irt} + u^-_{rt} \le c^t_{ijt} \quad \forall i\in M, j\in N, r\in R, \\ t\in\{1,2,\cdots,T\} \tag{43}$$

$$-p_{irt} - l^-_{jrt} + g_{irt} + u^-_{rt} \le c^t_{ijt} \quad \forall i\in M, j\in E, r\in R, \\ t\in\{1,2,\cdots,T\} \tag{44}$$

$$-f_{irt} + g_{irt} - g_{ir,t+1} \le c^s_{irt} \quad \forall i\in M, r\in R, \\ t\in\{1,2,\cdots,T-1\} \tag{45}$$

$$-f_{irT} + g_{irT} \le c^s_{irT} \quad \forall i\in M, r\in R \tag{46}$$

$$\begin{aligned} & e_{kt} - \sum_{t'=t}^{T} v^+_{jt'} n_{kt'} - s_{jkt} n_{kt} + \rho_{kt} \\ & - \sum_{r\in R} n_{kt}(\kappa^*_{rt} u^-_{rt} + o^-_{rt} - w^+_{rt}) \\ & \le Len_{jk} c^e_{jkt} n_{kt} \quad \forall k\in G, j\in N, t\in\{1,2,\cdots,T\} \end{aligned} \tag{47}$$

$$e_{kt} - \sum_{t'=t}^{T} v_{jt'}^{-} n_{kt'} - s_{jkt} n_{kt} + \rho_{kt} - \sum_{r\in R} n_{kt}(\kappa_{rt}^{*} u_{rt}^{-} + o_{rt}^{-} - w_{rt}^{+}) \le Len_{jk} c_{jkt}^{e} n_{kt} \quad \forall k \in G, j \in E, t \in \{1,2,\cdots,T\} \tag{48}$$

$$e_{kt} \le \tau_{kt} n_{kt} \quad \forall k \in G, t \in \{1,\cdots,T\} \tag{49}$$

$$u_{rt}^{-} - \gamma_{rt} u_{rt}^{+} = 0 \quad \forall r \in R, t \in \{1,2,\cdots,T\} \tag{50}$$

$$\kappa_{rt}^{*}(u_{rt}^{-} + o_{rt}^{+}) + o_{rt}^{-} - w_{rt}^{+} + w_{rt}^{-} - \Lambda_{rt} - \mu_{rt} u_{rt}^{+} = 0 \quad \forall r \in R, t \in \{1,2,\cdots,T\} \tag{51}$$

$$(\kappa_{rt}^{*} - \mu_{rt})(u_{rt}^{-} + o_{rt}^{+}) + o_{rt}^{-} - w_{rt}^{+} + w_{rt}^{-} - \Lambda_{rt} - \sigma_{rt} u_{rt}^{+} \le 0 \quad \forall r \in R, t \in \{1,2,\cdots,T\} \tag{52}$$

$$-(\kappa_{rt}^{*} - \mu_{rt})(u_{rt}^{-} + o_{rt}^{+}) - o_{rt}^{-} + w_{rt}^{+} - w_{rt}^{-} + \Lambda_{rt} - \sigma_{r}^{t} u_{rt}^{+} \le 0 \quad \forall r \in R, t \in \{1,2,\cdots,T\} \tag{53}$$

$$\sum_{t'=1}^{t}\sum_{r'\in R}(\kappa_{r't'}^{*} - \mu_{r't'})(u_{rt}^{-} + o_{rt}^{+}) + o_{rt}^{-} - w_{rt}^{+} + w_{rt}^{-} - \Lambda_{rt} + \Upsilon_{t}^{+} - \Upsilon_{t}^{-} - \xi_{t} u_{rt}^{+} \le 0 \quad \forall r \in R, t \in \{1,2,\cdots,T\} \tag{54}$$

$$-\sum_{t'=1}^{t}\sum_{r'=1}^{R}(\kappa_{r't'}^{*} - \mu_{r't'})(u_{rt}^{-} + o_{rt}^{+}) - o_{rt}^{-} + w_{rt}^{+} - w_{rt}^{-} + \Lambda_{rt} - \Upsilon_{t}^{+} + \Upsilon_{t}^{-} - \xi_{t} u_{rt}^{+} \le 0 \quad \forall r \in R, t \in \{1,2,\cdots,T\} \tag{55}$$

$$u_{rt}^{-} + o_{rt}^{+} - u_{rt}^{+} = 0 \qquad \forall r \in R, t \in \{1,2,\cdots,T\} \tag{56}$$

$$o_{rt}^{-} + w_{rt}^{+} - \zeta_{rt} u_{rt}^{-} \le 0 \qquad \forall r \in R, t \in \{1,2,\cdots,T\} \tag{57}$$

$$w_{rt}^{-} + \Lambda_{rt} - \zeta_{rt} o_{rt}^{+} \le 0 \qquad \forall r \in R, t \in \{1,2,\cdots,T\} \tag{58}$$

$$\Upsilon_{t}^{+} + \Upsilon_{t}^{-} - \sum_{r\in R}(u_{rt}^{-} + o_{rt}^{+}) \sum_{t'=1}^{t} \sum_{r'\in R,(r',t')\neq(r,t)} \zeta_{r't'} \le 0 \quad \forall t \in \{1,2,\cdots,T\} \tag{59}$$

$$p_{irt}, l_{jrt}^{+}, l_{jrt}^{-}, f_{irt}, v_{jt}^{+}, v_{jt}^{-}, s_{jkt}, u_{rt}^{+}, u_{rt}^{-}, o_{rt}^{+}, o_{rt}^{-}, w_{rt}^{+}, w_{rt}^{-}, \Lambda_{rt}, \Upsilon_{t}^{+}, \Upsilon_{t}^{-} \ge 0 \tag{60}$$

From constraints (50) and (56), we can obtain $u_{rt}^{-} = \gamma_{rt} u_{rt}^{+}$ and $u_{rt}^{-} + o_{rt}^{+} = u_{rt}^{+}$, and thus $o_{rt}^{+} = (1-\gamma_{rt}) u_{rt}^{+}$. Further by constraints (51), we have $(\kappa_{rt}^{*} - \mu_{rt})(u_{rt}^{-} + o_{rt}^{+}) + o_{rt}^{-} - w_{rt}^{+} + w_{rt}^{-} - \Lambda_{rt} = \mu_{rt} u_{rt}^{+} - \mu_{rt}(u_{rt}^{-} + o_{rt}^{+}) = 0$, implying that constraints (52) and (53) are redundant. Based on the above analysis, the *DSP* $(\bar{\mathbf{x}}, \bar{\mathbf{y}}, \bar{\mathbf{z}})$ can be reformulated as follows.

$$\begin{aligned} max\ & -\sum_{t=1}^{T}\sum_{i\in M}\sum_{r\in R} \bar{x}_{it} Q_{ir}^{d}(p_{irt} + f_{irt}) \\ & - \sum_{t=1}^{T}\sum_{j\in N}\sum_{r\in R} \bar{y}_{jt} Q_{j}^{ri} l_{jrt}^{+} - \sum_{t=1}^{T}\sum_{j\in E}\sum_{r\in R} Q_{j}^{ri} l_{jrt}^{-} \\ & + \sum_{t=1}^{T}\sum_{k\in G} e_{kt} + \sum_{t=1}^{T}\sum_{i\in M}\sum_{r\in R} \vartheta_{irt} g_{irt} \\ & - \sum_{t=1}^{T}\sum_{j\in N} \bar{y}_{jt} Q_{j}^{rh} v_{jt}^{+} - \sum_{t=1}^{T}\sum_{j\in E} Q_{j}^{rh} v_{jt}^{-} \\ & - \sum_{t=1}^{T}\sum_{j\in N\cup E}\sum_{k\in G} \bar{z}_{jkt} Q_{jk}^{c} s_{jkt} \\ & + \sum_{t=1}^{T}\sum_{k\in G} min\{1, \bar{\alpha}_{kt}(1+\epsilon_1)\}\rho_{kt} \end{aligned}$$

s.t. constraints (45), (46), (49), (54), (55) , (59),

$$-p_{irt} - l_{jrt}^{+} + g_{irt} + \gamma_{rt} u_{rt}^{+} \le c_{ijt}^{t} \quad \forall i \in M, j \in N, r \in R, t \in \{1,2,\cdots,T\} \tag{61}$$

$$-p_{irt} - l_{jrt}^{-} + g_{irt} + \gamma_{rt} u_{rt}^{+} \le c_{ijt}^{t} \quad \forall i \in M, j \in E, r \in R, t \in \{1,2,\cdots,T\} \tag{62}$$

$$e_{kt} - \sum_{t'=t}^{T} v_{jt'}^{+} n_{kt'} - s_{jkt} n_{kt} + \rho_{kt} - \sum_{r\in R} n_{kt}(\kappa_{rt}^{*}\gamma_{rt} u_{rt}^{+} + o_{rt}^{-} - w_{rt}^{+}) \le Len_{jk} c_{jkt}^{e} n_{kt} \quad \forall k \in G, j \in N, t \in \{1,2,\cdots,T\} \tag{63}$$

$$e_{kt} - \sum_{t'=t}^{T} v_{jt'}^{-} n_{kt'} - s_{jkt} n_{kt} + \rho_{kt} - \sum_{r\in R} n_{kt}(\kappa_{rt}^{*}\gamma_{rt} u_{rt}^{+} + o_{rt}^{-} - w_{rt}^{+}) \le Len_{jk} c_{jkt}^{e} n_{kt} \quad \forall k \in G, j \in E, t \in \{1,2,\cdots,T\} \tag{64}$$

$$(\kappa_{rt}^{*} - \mu_{rt}) u_{rt}^{+} + o_{rt}^{-} - w_{rt}^{+} + w_{rt}^{-} - \Lambda_{rt} = 0 \quad \forall r \in R, t \in \{1,2,\cdots,T\} \tag{65}$$

$$o_{rt}^{-} + w_{rt}^{+} - \zeta_{rt}\gamma_{rt} u_{rt}^{+} \le 0 \quad \forall r \in R, t \in \{1,2,\cdots,T\} \tag{66}$$

$$w_{rt}^{-} + \Lambda_{rt} - \zeta_{rt}(1-\gamma_{rt}) u_{rt}^{+} \le 0 \quad \forall r \in R, t \in \{1,2,\cdots,T\} \tag{67}$$

$$p_{irt}, l^{+}_{jrt}, l^{-}_{jrt}, f_{irt}, v^{+}_{jt}, v^{-}_{jt}, s_{jkt}, u^{+}_{rt}, u^{-}_{rt}, o^{+}_{rt}, o^{-}_{rt}, w^{+}_{rt}, w^{-}_{rt}, \Lambda_{rt},$$
$$\Upsilon^{+}_{t}, \Upsilon^{-}_{t} \geq 0 \tag{68}$$

Let *EP* and *ER* be the sets of extreme points and extreme rays of the feasible set of DSP $(\bar{x}, \bar{y}, \bar{z})$, respectively, both of which do not depend on $\bar{x}, \bar{y}$, and $\bar{z}$. The *MP* can be equivalently reformulated as follows:

$$\min \sum_{t=1}^{T} \sum_{i \in M} f^{d}_{it} x_{it} + \sum_{t=1}^{T} \sum_{j \in N} f^{r}_{jt} y_{jt} + D$$

Subject to Constraints (4), (5), (16), (17)

$$\begin{aligned} D \geq & - \sum_{t=1}^{T} \sum_{i \in M} \sum_{r \in R} x_{it} Q^{d}_{ir} (p_{irt} + f_{irt}) \\ & - \sum_{t=1}^{T} \sum_{j \in N} \sum_{r \in R} y_{jt} Q^{ri}_{j} l^{+}_{jrt} - \\ & \sum_{t=1}^{T} \sum_{j \in E} \sum_{r \in R} Q^{ri}_{j} l^{-}_{jrt} + \sum_{t=1}^{T} \sum_{k \in G} e_{kt} + \sum_{t=1}^{T} \sum_{i \in M} \sum_{r \in R} \vartheta_{irt} g_{irt} \\ & - \sum_{t=1}^{T} \sum_{(j \in N)} y_{j}t Q^{rh}_{j} h v^{+}_{jt} \sum_{t=1}^{T} \sum_{(j \in E)}^{T} Q^{rh}_{j} h v^{-}_{jt} \\ & - \sum_{t=1}^{T} \sum_{(j \in N \cup E)} \sum_{(k \in G)} Z_{jkt} Q^{c}_{jk} s_{jkt} \\ & + \sum_{t=1}^{T} \sum_{k \in G} \min\{1, \bar{\alpha}_{kt}(1 + \epsilon_1)\} \rho_{kt}, \\ & \forall (p, l^{+}, l^{-}, f, \boldsymbol{e}, \boldsymbol{g}, \boldsymbol{v}^{+}, \boldsymbol{v}^{-}, \boldsymbol{s}, \boldsymbol{\rho}, \boldsymbol{u}^{+}, \boldsymbol{o}^{+}, \\ & \boldsymbol{w}^{+}, \boldsymbol{w}^{-}, \boldsymbol{\Upsilon}^{+}, \boldsymbol{\Upsilon}^{-}) \in EP \end{aligned} \tag{69}$$

$$\begin{aligned} 0 \geq & - \sum_{t=1}^{T} \sum_{i \in M} \sum_{r \in R} x_{it} Q^{d}_{ir} (p_{irt} + f_{irt}) \\ & - \sum_{t=1}^{T} \sum_{j \in N} \sum_{r \in R} y_{jt} Q^{ri}_{j} l^{+}_{jrt} - \sum_{t=1}^{T} \sum_{j \in E} \sum_{r \in R} Q^{ri}_{j} l^{-}_{jrt} \\ & + \sum_{t=1}^{T} \sum_{k \in G} e_{kt} + \sum_{t=1}^{T} \sum_{i \in M} \sum_{r \in R} \vartheta_{irt} g_{irt} \\ & - \sum_{t=1}^{T} \sum_{j \in N} y_{jt} Q^{rh}_{j} v^{+}_{jt} - \sum_{t=1}^{T} \sum_{j \in E} Q^{rh}_{j} v^{-}_{jt} \\ & - \sum_{t=1}^{T} \sum_{(j \in N \in E)} \sum_{(k \in G)} z_{j}kt Q_{j} k^{c} s_{j} kt \\ & + \sum_{(t=1)}^{T} \sum_{(k \in G)} min\{1, \alpha_{kt}(1 + \epsilon_1) \rho_{kt}, \end{aligned} \tag{70}$$

$$\forall (\boldsymbol{p}, \boldsymbol{l}^{+}, \boldsymbol{l}^{-}, \boldsymbol{f}, \boldsymbol{e}, \boldsymbol{g}, \boldsymbol{v}^{+}, \boldsymbol{v}^{-}, \boldsymbol{s}, \boldsymbol{\rho}, \boldsymbol{u}^{+}, \boldsymbol{o}^{+}, \boldsymbol{w}^{+}, \boldsymbol{w}^{-}, \boldsymbol{\Upsilon}^{+}, \boldsymbol{\Upsilon}^{-}) \in ER \tag{70}$$

$$x_{it}, y_{jt}, z_{jkt} \in \{0, 1\}, D \geq 0 \tag{71}$$

4.1.2. Basic benders decomposition algorithm

Let *UB* and *LB* be the current upper and lower bounds on the optimal solution value. Let l the current iteration number, and z^{l}_{DS} the optimal value of the dual subproblem at iteration l. We refer to the *MP* with *EP* and *ER* being replaced with their subsets as the relaxed *MP*. The MP is initially relaxed with $EP = ER = \emptyset$. In each iteration, we first obtain the optimal solution $(\bar{x}, \bar{y}, \bar{z}, \bar{D})$ of the relaxed *MP*, and then solve the resulting dual subproblem *DS* $(\bar{x}, \bar{y}, \bar{z})$ to obtain the optimal solution $(\boldsymbol{p}, \boldsymbol{l}^{+}, \boldsymbol{l}^{-}, \boldsymbol{f}, \boldsymbol{e}, \boldsymbol{g}, \boldsymbol{v}^{+}, \boldsymbol{v}^{-}, \boldsymbol{s}, \boldsymbol{\rho}, \boldsymbol{u}^{+}, \boldsymbol{o}^{+}, \boldsymbol{w}^{+}, \boldsymbol{w}^{-}, \boldsymbol{\Upsilon}^{+}, \boldsymbol{\Upsilon}^{-})$ with optimal value z_{DS}. If the dual subproblem *DS* $(\bar{x}, \bar{y}, \bar{z})$ is unbounded, we add the following Benders feasibility cut

$$\begin{aligned} 0 \geq & - \sum_{t=1}^{T} \sum_{i \in M} \sum_{r \in R} x_{it} Q^{d}_{ir} (p_{irt} + f_{irt}) \\ & - \sum_{t=1}^{T} \sum_{j \in N} \sum_{r \in R} y_{jt} Q^{ri}_{j} l^{+}_{jrt} - \sum_{t=1}^{T} \sum_{j \in E} \sum_{r \in R} Q^{ri}_{j} l^{-}_{jrt} \\ & + \sum_{t=1}^{T} \sum_{k \in G} e_{kt} + \sum_{t=1}^{T} \sum_{i \in M} \sum_{r \in R} \vartheta_{irt} g_{irt} \\ & - \sum_{t=1}^{T} \sum_{j \in N} y_{jt} Q^{rh}_{j} v^{+}_{jt} - \sum_{t=1}^{T} \sum_{j \in E} Q^{rh}_{j} v^{-}_{jt} \\ & - \sum_{t=1}^{T} \sum_{j \in N \cup E} \sum_{k \in G} z_{jkt} Q^{c}_{jk} s_{jkt} \\ & + \sum_{t=1}^{T} \sum_{k \in G} min\{1, \bar{\alpha}_{kt}(1 + \epsilon_1)\} \rho_{kt} \end{aligned}$$

to the relaxed *MP*. Otherwise, if the dual subproblem *DS* $(\bar{x}, \bar{y}, \bar{z})$ is bounded, but $z_{DS} < \bar{D}$, we add the following Benders optimality cut

$$\begin{aligned} D \geq & - \sum_{t=1}^{T} \sum_{i \in M} \sum_{r \in R} x_{it} Q^{d}_{ir} (p_{irt} + f_{irt}) \\ & - \sum_{t=1}^{T} \sum_{j \in N} \sum_{r \in R} y_{jt} Q^{ri}_{j} l^{+}_{jrt} - \sum_{t=1}^{T} \sum_{j \in E} \sum_{r \in R} Q^{ri}_{j} l^{-}_{jrt} \\ & + \sum_{t=1}^{T} \sum_{k \in G} e_{kt} + \sum_{t=1}^{T} \sum_{i \in M} \sum_{r \in R} \vartheta_{irt} g_{irt} \end{aligned}$$

$$
\begin{aligned}
&- \sum_{t=1}^{T} \sum_{j \in N} y_{jt} Q_j^{rh} v_{jt}^{+} - \sum_{t=1}^{T} \sum_{j \in E} Q_j^{rh} v_{jt}^{-} \\
&- \sum_{t=1}^{T} \sum_{j \in N \cup E} \sum_{k \in G} z_{jkt} Q_{jk}^{c} s_{jkt} \\
&+ \sum_{t=1}^{T} \sum_{k \in G} min\{1, \bar{\alpha}_{kt}(1+\epsilon_1)\} \rho_{kt}
\end{aligned}
$$

to the relaxed *MP*. An upper bound can be computed from the feasible subproblem and a lower bound is obtained if the master problem is solved to optimality. The process continues until the lower and upper bounds are sufficiently close. The framework of the basic Benders decomposition algorithm is given in Algorithm 1 in Appendix 2.

4.2. Algorithm enhancements

The computational efficiency of the Benders decomposition algorithm strongly depends on the quality of the generated Benders cuts. Generally, the better the quality of the Benders cuts, the fewer iterations are required to solve the *MP*. However, there may be multiple optimal solutions when the dual subproblem is solved, each of which may yield a Benders cut. In order to generate better Benders cuts, we employ the following two algorithm enhancements: (i) In–out Benders cut generation; and (ii) Initial cut generation.

4.2.1. In–out benders cut generation strategy

The in–out Benders cut generation strategy, which was first developed by Ben-Ameur and Neto (2007), can generate more effective cuts, which has been proven to an effective strategy to speed up the convergence of Benders decomposition algorithm (Fischetti, Ljubic, and Sinnl 2016; Yang et al. 2023).

The idea of in–out column generation strategy is as follows. In each iteration, we get two points: one is the optimal solution of the relaxed *MP*, denoted as $(\boldsymbol{x}_{out}, \boldsymbol{y}_{out}, \boldsymbol{z}_{out})$, and the other is the feasible solution of the *MP*, denoted as $(\boldsymbol{x}_{in}, \boldsymbol{y}_{in}, \boldsymbol{z}_{in})$. When solving the dual subproblem to generate Benders cuts, instead of $(\boldsymbol{x}_{out}, \boldsymbol{y}_{out}, \boldsymbol{z}_{out})$, we employ an intermediate point (separation point), descripted as $(\boldsymbol{x}_{sep}, \boldsymbol{y}_{sep}, \boldsymbol{z}_{sep}) = \varphi(\boldsymbol{x}_{in}, \boldsymbol{y}_{in}, \boldsymbol{z}_{in}) + (1-\varphi)(\boldsymbol{x}_{out}, \boldsymbol{y}_{out}, \boldsymbol{z}_{out})$, to find Benders cuts, where $\varphi \in \{0, 1\}$ is a real valued scalar.

If valid Benders cuts are found, which are also violated by $(\boldsymbol{x}_{out}, \boldsymbol{y}_{out}, \boldsymbol{z}_{out})$ due to the definition of $(\boldsymbol{x}_{sep}, \boldsymbol{y}_{sep}, \boldsymbol{z}_{sep})$, we add them to the relaxed *MP*. By solving the resulting relaxed *MP*, we yield a new point $(\boldsymbol{x}_{out}, \boldsymbol{y}_{out}, \boldsymbol{z}_{out})$ and keep $(\boldsymbol{x}_{in}, \boldsymbol{y}_{in}, \boldsymbol{z}_{in})$ unchanged. If no Benders cuts are found, we update $(\boldsymbol{x}_{in}, \boldsymbol{y}_{in}, \boldsymbol{z}_{in})$ as $(\boldsymbol{x}_{sep}, \boldsymbol{y}_{sep}, \boldsymbol{z}_{sep})$ and keep $(\boldsymbol{x}_{out}, \boldsymbol{y}_{out}, \boldsymbol{z}_{out})$ unchanged. This process continues until the optimality gap is equal to or lower than lower than a given precision. In our implementation, we only apply this in–out Benders cut generation strategy at the root node.

4.2.2. Initial cut generation strategy

Magnanti and Wong (1981) propose a new strong cuts strategy, denoted as MW method, to generate the Pareto-optimal cuts by solving an auxiliary dual subproblem. Papadakos (2008) points out that the MW method is shown to exhibit difficulties due to its dependence on the subproblem, and an independent version is therefore introduced, called enhanced MW method, and denoted as EMW. However, both MW and EMW methods need to solve the dual subproblem and an auxiliary subproblem, which consumes a lot of CPU time. As mentioned in Bayram and Yaman (2018), for both algorithms, the number of iterations and the total number of resulting optimality cuts are generally reduced over the Benders decomposition algorithm. However, CPU time deteriorates due to solving the dual subproblem and the MW auxiliary problem in each iteration. It is worth noting that the EMW problem is independent of the subproblem, so we can take advantage of adding initial cuts to the *MP* before we begin solving it. We denote this strategy as the initial cut generation strategy.

Specifically, we find the Magnanti-Wong points $(\boldsymbol{x}_0, \boldsymbol{y}_0, \boldsymbol{z}_0)$, and solve the independent Magnanti-Wong problems $DSP(\boldsymbol{x}_0, \boldsymbol{y}_0, \boldsymbol{z}_0)$ to obtain $(\boldsymbol{p}_0, \boldsymbol{l}_0^{+}, \boldsymbol{l}_0^{-}, \boldsymbol{f}_0, \boldsymbol{e}_0, \boldsymbol{g}_0, \boldsymbol{p}_0, \boldsymbol{v}_0^{+}, \boldsymbol{v}_0^{-}, \boldsymbol{e}_0, \boldsymbol{e}_0, \boldsymbol{s}_0, \boldsymbol{\rho}_0, \boldsymbol{u}_0^{+}, \boldsymbol{o}_0^{+}, \boldsymbol{w}_0^{+}, \boldsymbol{w}_0^{-}, \boldsymbol{\gamma}_0^{+}, \boldsymbol{\gamma}_0^{-})$. We generate some initial Benders cuts with one iteration only based the solutiTon to the $DSP(\boldsymbol{x}_0, \boldsymbol{y}_0, \boldsymbol{z}_0)$, and then continue the basic Benders decomposition algorithm. In this paper, we first explore the heuristic by fixing some binary variables $\bar{x}_{it}, \bar{y}_{jt}$, and $\bar{z}_{jkt}$ as 1 to obtain some feasible first-stage solutions $(\boldsymbol{x}_0, \boldsymbol{y}_0, \boldsymbol{z}_0)$ of the *D-MILP*, and then use these first-stage solutions as the Magnanti-Wong point to generate the initial set of cuts.

4.3. Branch-and benders-cut algorithm

In branch-and-Benders-cut algorithm, the Benders decomposition procedure is implemented in the framework of the branch and cut, where the Benders subproblems are solved at each node in the search tree via callback functionality of CPLEX. Specifically, we first develop a simple greedy heuristic, where distribution centres and rescue shelters are opened one by one in each period to satisfy the demand of injured people, to find a feasible first-stage solution $(\boldsymbol{x}_{in}, \boldsymbol{y}_{in}, \boldsymbol{z}_{in})$ to the *MP* with corresponding upper bound *UB*. During the iterative phase of the

algorithm, before solving the relaxed *MP*, we deal with an independently dual subproblem only once to generate an initial set of valid cuts, and add these cuts to the relaxed *MP*. Then, if the stopping criterion is not meet, based on the feasible solution ($\boldsymbol{x}_{in}$, $\boldsymbol{y}_{in}$, $\boldsymbol{z}_{in}$), the optimal solution search process is carried out at the root node with no branch requirement, we solve the relaxed *MP* and execute the in–out Benders cut generation. Thus, we can obtain violated Benders cuts by solving dual subproblem with separation point (x_{sep}, y_{sep}, z_{sep}), and add these cuts to the relaxed *MP*. The addition of these lazy cuts is implemented within a LazyConstraintCallback routine that takes the form of CPXcutcall-Backadd in CPLEX.

5. Numerical results

We construct extensive numerical experiment to test our model and solution algorithm from the following aspects: (i) prove the superiority of the *DRM* over the deterministic model (*DM*) and stochastic model (*SM*); (ii) verify the effectiveness of the algorithm enhancements and the computational efficiency of the proposed algorithm; (iii) demonstrate the benefit of our integrated solution approach over a sequential solution approach (injured people evacuation first, relief supplies allocation second); (iv) ascertain the impacts of some model parameters on the solution structure.

All algorithms are coded in Java and the linear programming model is solved by CPLEX 12.8. All runs were performed on a computer with a 64-bit 2.4 GHz Intel Core processor and 8 GB of RAM.

5.1. Instance generation

For all we know, no standard test datasets can be directly obtained for the disaster relief model we consider. Thus, according to some existing works about disaster relief (Dalal and Üster 2018; Bayram and Yaman 2018; Üster and Dalal 2017, Liu et al., 2019), we generate our problem instances with some reasonable modifications.

For extensive analysis, we conduct experiments with instances with different sizes. Specifically, we consider $|I| \in \{40, 50, 60\}$, $|J_n| \in \{40, 50, 60\}$, $|J_e| = 0.4|J_n|$, $|G| \in \{60, 80, 100, 120\}$, $|T| \in \{1, 3\}$, and, $|R| = 4$. We set the main parameters as follows.

(i) Referring to Üster and Dalal (2017), the total number of injured people at affected area k during time period t, n_{kt} follows a uniform distribution $U[250, 600]$.

(ii) According to Dalal and Üster (2018), to meet the needs of all casualties as much as possible in each time period, the maximum inventory capacity of relief supplies r at emergency relief distribution centre i, Q^d_{ir} is set to $\max\limits_t \left(\max\limits_l (\tilde{\kappa}^l_{rt}) \frac{\sum_{k\in G} n_{kt} \times U[0.75,0.95]}{\omega \times |I|} \right)$ depending on the total number of injured people and the maximum demand, where $\propto$ is set to 0.2. Similarly, the maximum inventory capacity Q^{ri}_j for relief supplies and the maximum holding capacity Q^{rh}_j for injured people of rescue shelter j are set to $\max\limits_t \left(\max\limits_r \left(\frac{\sum_{i\in I} Q^d_{ir} \times U[2,4]}{|J|} \right) \right)$ and $\max\limits_t \left(\frac{\sum_{k\in G} n_{kt} \times U[2,4]}{|J|} \right)$, respectively, and the capacity of the arc between affected area k and rescue shelter j, Q^c_{jk} is set to $\max\limits_t \left(\frac{\sum_{k\in G} n_{kt} \times U[4,6]}{|G| \times |J|} \right)$. The amount of relief supplies r supplied by the suppliers to distribution centre i, ϑ_{irt} is set to $Q^d_{ir} \times U[0.75, 0.95]$.

(iii) Referring to Dalal and Üster (2018), in each time period $t \in \{1, 2, \ldots, T\}$, the unit transportation cost from distribution centre i to rescue shelter j, c^t_{ijt} follows a uniform distribution $U[0.1, 0.2]$, the evacuation cost per distance c^e_{jkt} follows a uniform distribution $U[0.01, 0.05]$, and the unit storage cost c^s_{irt} follows a uniform distribution $U[2, 4]$, and the fixed open costs of distribution centre i and rescue shelter j, f^d_{it} and f^r_{jt}, follow uniform distributions $U[30, 60]$ and $U[50, 100]$, respectively.

(iv) The unit penalty cost of non-evacuees τ_{kt} should not be higher than the maximum transportation cost and not less than the minimum transportation cost, which follows a uniform distribution $U[\partial c^-, \partial c^+]$, where $c^- = \min_{k,j,t} Len_{jk} c^e_{jkt}$ and $c^+ = \max_{k,j,t} Len_{jk} c^e_{jkt}$ denote the minimum transportation cost and maximum transportation cost, respectively, and $\partial \in \{0, 1\}$ is pre-set to 0.6. The maximum evacuation distance ϖ is set to $\max\limits_{k,j} Len_{jk} \times U[0.6, 0.8]$. Here, the distance between two nodes in rescue network design, say Len_{jk} and Len_{ij}, is measured by Euclidean distance.

(v) On the basis of the available supplies and willingness to evacuate, the nominal value of evacuee fraction at affected area k, $\bar{\alpha}_{kt}$ follows a uniform distribution $U[0.7, 0.8]$, and the uncertainty measure $\epsilon_1 \in [0, 1]$ is set to 0.05.

As for the definition of distributional ambiguity sets, we assume the uncertain parameter $\tilde{\boldsymbol{\kappa}}$ satisfies the following assumptions.

(i) We pack the relief supplies into a bundle, convert it into volume units, and set the unit demand of

injuries for relief supplies $r \in R$ during time period t, $\tilde{\kappa}_{rt}$ follows a uniform distribution $U[3, 6]$.

(ii) We randomly generate 1000 training samples $\{\tilde{\boldsymbol{\kappa}}^l\}_{l=1}^{1000}$, to form the sample distribution. Thus, the parameters $\boldsymbol{\mu}$, $\boldsymbol{\sigma}$, and ξ_t are set to $\frac{1}{1000}\sum_{l=1}^{1000}\tilde{\boldsymbol{\kappa}}^l$, $\frac{1}{1000g}\sum_{l=1}^{1000}|\tilde{\boldsymbol{\kappa}}^l - \boldsymbol{\mu}|$, and $\frac{1}{1000g}\sum_{l=1}^{1000}\left|\sum_{l=1}^{t}1'(\tilde{\boldsymbol{\kappa}}^l - \boldsymbol{\mu}^l)\right|$, where g is a positive parameter set to 2.

(iii) The lower and upper bounds of $\tilde{\boldsymbol{\kappa}}$ are set to $\min_l\{\tilde{\boldsymbol{\kappa}}^l\}_{l=1}^{1000}$ and $\max_l\{\tilde{\boldsymbol{\kappa}}^l\}_{l=1}^{1000}$, respectively, and $\gamma_{rt} = \gamma$ is set to 0.01.

For each instance size $(|I|, |J_n|, |G|)$, we randomly generate 20 instances. Thus, we have 720 instances in total.

5.2. Benefit of considering uncertainty and distributional robustness

In this section, we evaluate the performance of the *DRM* by comparing with the *DM* and *SM* through out-of-sample analysis. The *DM* use nominal demands $\boldsymbol{\mu}$ with no uncertainty, and *SM* is constructed by sample average approximation (SAA) method, which approximates the expected demands by the average demands under the sample distribution. The detailed description of the *SM* is shown in Appendix 3. To get efficient comparison results in reasonable CPU time, we focus on the instances with $|I| = 60, |J_n| = 60, |G| = 60$ and $|T| = 1$, and randomly choose 500 samples from the 1000 training samples to construct the *DRM* and *SM*. For out-of-sample analysis, we randomly generate 10,000 samples in a similar manner to Section 5.1.1 and evaluate the performance of the first-stage solutions $(\boldsymbol{x}, \boldsymbol{y}, \boldsymbol{z})$ obtained from the *DRM*, *DM*, and *SM*. Specifically, for each feasible first-stage solution $(\boldsymbol{x}, \boldsymbol{y}, \boldsymbol{z})$, we calculate the sum of the storage and transportation costs of relief supplies, evacuation cost of injured people, and penalty cost of non-evacuees for each scenario under the first stage solution $(\boldsymbol{x}, \boldsymbol{y}, \boldsymbol{z})$ and then summarise various statistics of the resulting values above to analyse the effectiveness and robustness of the given solution.

The detailed results are summarised in Table 4. Here, we report the average total cost (ATC) of each comparison model, the average out-of-sample total cost (AOTC) with corresponding standard deviation (OSD) for feasible samples under the first-stage solution, and the probability of distributionally robust chance constraint violation (Risk) which measures the relative frequency of infeasible samples over 10,000 out-of-sample under the first-stage solution. Figure 2 describes the out-of-sample total cost (OTC) histograms of the comparison models for the feasible out-of-samples.

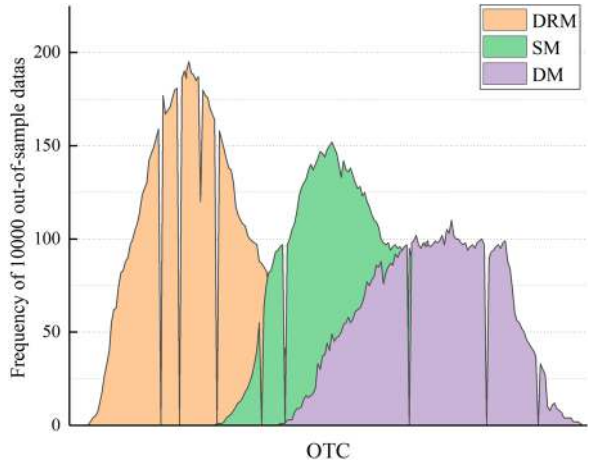

Figure 2. Histograms of OTC of the DRM, SM and DM for the feasible out-of-samples.

Table 3. Comparison results of the *DRM*, *SM* and *DM*.

Model	ATC	AOTC	OSD	Risk (%)
DRM	1060257.307	1817134.1	7845.2	0.0
SM	1053470.102	1823221.2	7876.3	2.9
DM	1051393.753	1828379.4	7938.6	46.8

From the first two columns of Table 3, we can see that the *DRM* leads to more conservative solutions than the DM and SM, which yields the largest ATC, followed by the *SM*. These observations are consistent with our expectation, since the *DRM* aims at minimising the total cost under more compact distributionally robust chance constraints, and the *SM* minimises the total cost under the constraints that the amount of emergency supplies delivered to rescue shelters in each time period is no less than the demand under all the 500 training samples. However, the *DRM* is not too conservative, which only increases ATC by 0.64% over *SM*.

However, Figure 2 and the third to fifth columns of Table 3 demonstrate that the *DRM* performs best in all metrics related to out-of-sample test. Indeed, the *DRM* yields the least average out-of-sample total cost 1817134.1 with least standard deviation 7845.2, while the average out-of-sample total costs obtained from the *SM* and *DM* are 1823221.2 and 1828379.4 with standard deviations 7876.3 and 7938.6, respectively. These observations show that ignoring uncertainty during the design phase could lead to significant cost increase when they do happen, and that considering distributionally robustness yields the lest cost when encountering uncertainty. More importantly, the Risk achieved by the *DRM* is 0.00%, indicating that all 10,000 samples out of the first-stage

solution obtained from the *DRM* are feasible. In contrast, the Risks obtained from the *SM* and *DM* are 2.9% and 46.7%, respectively. These observations show that the *DRM* can effectively reduce the risk of system being 'unreliable'.

In sum, the above results obviously highlight the robustness and superiority of the *DRM*, which provides more reliable and flexible solutions that perform the best when faced uncertainty, followed by the *SM*.

5.3. Algorithm performance

In this section, we evaluate the effectiveness of the algorithm enhancements and the efficiency of the proposed algorithm. It mainly includes the comparison of the following versions: (i) solving the *D-MILP* using CPLEX without any brand and benders cut (CPLEX); (ii) The basic Branch-and-Benders-cut algorithm without any algorithm enhancement (BBC-B); (iii) the basic Branch-and-Benders-cut algorithm with in–out Benders cut generation strategy (BBC-IO); (iv) the basic Branch-and-Benders-cut algorithm with initial cut generation strategy (BBC-IC); and (v) the Branch-and-Benders-cut algorithm we develop (BBC-All). The time limit for each run of these algorithms is set to 5400 s.

The detailed comparison results are shown in Table 4. For each instance size, column 'NU' counts the number of 20 instances solved to optimality within the time limit, column 'ATimes' indicates the average CPU time spent in solving the instances that can be solved to optimality within the time limit; column 'ANodes' represents the average number of branch nodes explored; and column 'Gap (%)' indicates the average optimality gap among the unsolved instances, which can be calculated as $(UB - LB)/UB$, where UB and LB are the best upper and lower bounds obtained up to time limit. We also report the average value or total number of each metric ('Ave/Toa'), and use the symbol '-' to denote the case that all instances run out of memory.

Moreover, when the in–out Benders cut generation strategy is implemented, we set $\varphi = 0.9$, which is the best choice comparing with other alternative values through preliminary experiment. The detailed analysis results are given in Appendix 4.

The effectiveness of the algorithm enhancements. The results in Table 4 clearly demonstrate that the algorithm enhancements are very effective to enhance the performance of the proposed algorithm. Specifically, we can draw the following conclusions: (i) with more instances solved to optimality and less CPU time, the algorithm enhancements are all valid and complement each other; (ii) considering the marginal contribution to algorithmic performance, the in–out Benders cut generation strategy seems to be better than the initial cut generation strategy; and (iii) comparing with single strategy, using both strategies together results in the largest enhancement in algorithm performance. Indeed, from the column 'NU', we can see that BBC-B can only solve 683, the BBC-IO and BBC-IC are capable of solving 688 and 686, respectively, whereas our BBC-All can solve 703 out of the 720 instances to optimality within the time limit. Moreover, for the unsolved instances, the average optimality gaps obtained from the BBC-IO and BBC-IC are smaller than that obtained from the BBC-B. Regard to the CPU time, taking the instances with $|I| = 50$ as example, using only in–out column generation strategy, only initial cut generation strategy, and both strategies reduce the average CPU time by up to 29.62%, 23.83%, and 41.99% on average, respectively, over the baseline. The possible reason behind this observation is that adding the algorithm enhancements can tight the lower bound, and thus reducing the number of search nodes explored which can be verified from the column 'ANodes'.

Comparison with CPLEX. The results in Table 4 allow us to conclude with the following observations: (i) the average quality of solutions found by CPLEX is quite good for small-scale instances, while the performance of CPLEX deteriorates as the problem size increases; (ii) BBC-All yields stable results for all the test instances, and outperforms CPLEX when increasing the problem size. Although CPLEX is capable of optimality solving all the 240 instances with $|I| = 40$ and takes less CPU time compared to BBC-All, BBC-All is superior to CPLEX when $|I| = 60$, or $|I| = 50$ and $|J_n| \geq 50$, which solves more instances than CPLEX and takes much less CPU time when compared to the same instances. Most importantly, CPLEX cannot solve any instance due to out of memory, when $|I| = 60$, $|J_n| \geq 50$, and $|G| = 120$. These results clearly highlight the superiority of our proposed algorithm, and reveals the limitations of using a general-purpose solver to solve our problem.

5.4. Benefit of integrated solution approach

In this section, we show the cost savings that can be attained by solving the DRHND-FLRIAEP in an integrated fashion compared with a sequential solution approach. In the sequential solution approach, we first solve the evacuation planning problem, which contains only the opening variables of new rescue shelters $\boldsymbol{y} = (y_{jt})_{j\in N, t\in\{1,2,\cdots,T\}}$, the evacuation variables $\boldsymbol{z} = (z_{jkt})_{k\in G, j\in N\cup E, t\in\{1,2,\cdots,T\}}$, the evacuation percentage variables $\boldsymbol{h} = (h_{jkt})_{k\in G, j\in N\cup E, t\in\{1,2,\cdots,T\}}$ and the unevacuated percentage variables $\boldsymbol{\Delta} = (\Delta_{kt})_{k\in G, t\in\{1,2,\cdots,T\}}$, and the constraint sets (4b), and (4h)–(4n). Given the optimal solution to the evacuation planning problem, we

Table 4. Comparison results of algorithm performance.

Instances			CPLEX				BBC-B				BBC -IO				BBC -IC				BBC-All			
$\|I\|$	$\|J_n\|$	$\|G\|$	ATimes	ANodes	Gap (%)	NU	ATimes	ANodes	Gap (%)	NU	ATimes	ANodes	Gap (%)	NU	ATimes	ANodes	Gap (%)	NU	ATimes	ANodes	Gap (%)	NU
40	40	60	72.8	58.2	0	0	424.3	565.5	0	0	374.7	198.1	0	0	414.7	218.0	0	0	264.6	142.7	0	0
		80	139.0	78.1	0	0	679.4	929.1	0	0	623.4	250.8	0	0	628.4	549.9	0	0	420.1	196.2	0	0
		100	260.1	140.2	0	0	1019.2	1133.2	0	0	898.5	561.6	0	0	913.8	681.4	0	0	662.7	506.4	0	0
		120	417.7	241.6	0	0	1428.9	1208.6	0	0	1176.6	642.7	0	0	1161.7	843.9	0	0	753.5	587.5	0	0
		Ave/Toa	222.4	129.5	0	0	888.0	959.1	0	0	768.3	413.3	0	0	779.7	573.3	0	0	525.2	358.2	0	0
	50	60	144.0	138.4	0	0	576.3	655.1	0	0	494.6	322.4	0	0	495.0	384.8	0	0	364.9	266.6	0	0
		80	378.1	305.9	0	0	1049.7	946.4	0	0	877.1	607.4	0	0	899.1	791.2	0	0	798.4	552.2	0	0
		100	711.6	1010.9	0	0	1910.8	1159.8	0	0	1587.3	1112.5	0	0	1613.1	1115.5	0	0	1231.8	1057.6	0	0
		120	1209.6	989.5	0	0	2793.4	1635.7	0	0	2183.6	1491.9	0	0	2220.7	1542.3	0	0	1929.8	1435.7	0	0
		Ave/Toa	610.8	611.2	0	0	1582.6	1099.3	0	0	1285.7	883.6	0	0	1307.0	958.5	0	0	1081.2	828.0	0	0
	60	60	639.4	547.1	0	0	1016.5	905.9	0	0	893.6	647.1	0	0	908.0	746.5	0	0	719.1	592.2	0	0
		80	1230.7	977.2	0	0	1756.1	1162.8	0	0	1473.8	1127.0	0	0	1567.3	1078.2	0	0	1310.9	1022.6	0	0
		100	2007.0	1079.9	0	0	2789.1	1347.5	0	0	2197.9	1141.2	0	0	2515.9	1163.6	0	0	2027.3	1086.4	0	0
		120	2689.0	1492.4	0	0	3797.0	1868.7	0	0	3103.5	1635.1	0	0	3114.7	1748.0	0	0	2778.4	1580.1	0	0
		Ave/Toa	1641.5	1024.2	0	0	2339.7	1321.2	0	0	1917.2	1137.6	0	0	2026.5	1184.1	0	0	1708.9	1070.3	0	0
50	40	60	411.0	387.4	0	0	665.5	776.4	0	0	563.7	488.9	0	0	546.1	511.9	0	0	390.9	433.5	0	0
		80	512.6	680.1	0	0	869.0	1149.8	0	0	665.6	681.7	0	0	665.6	770.3	0	0	504.3	626.0	0	0
		100	874.9	979.8	0	0	1304.6	1471.9	0	0	868.3	981.8	0	0	980.1	1137.2	0	0	795.5	926.6	0	0
		120	1138.4	1255.7	0	0	2005.0	1890.2	0	0	1323.4	1257.8	0	0	1507.4	1326.6	0	0	1136.0	1202.0	0	0
		Ave/Toa	734.2	825.8	0	0	1211.0	1322.1	0	0	855.3	852.6	0	0	924.8	936.5	0	0	706.7	797.0	0	0
	50	60	775.4	773.1	0	0	1245.9	989.7	0	0	790.4	773.3	0	0	938.0	808.6	0	0	655.6	718.1	0	0
		80	1338.8	935.0	0	0	2110.7	1340.7	0	0	1375.6	1037.7	0	0	1404.5	1093.3	0	0	1159.2	982.3	0	0
		100	2722.7	1470.0	0	0	2760.8	1772.3	0	0	2269.0	1271.3	–	0	2201.4	1331.3	0	0	1844.1	1216.9	0	0
		120	3540.4	2081.5	1.46	2	3826.6	1980.7	0	0	3164.0	1551.1	0	0	3060.1	1556.2	0	0	2675.6	1495.3	0	0
		Ave/Toa	2094.3	1314.9	1.46	2	2486.0	1520.9	0	0	1899.8	1158.4	0	0	1901.0	1197.4	0	0	1583.6	1103.2	0	0
	60	60	1551.2	1082.7	0	0	1717.0	1071.6	0	0	1315.5	892.2	0	0	1492.1	948.4	0	0	1271.8	837.3	0	0
		80	2909.8	1509.2	0	0	3266.6	1650.3	0	0	2942.5	1451.4	0	0	2824.4	1411.2	0	0	2330.7	1355.8	0	0
		100	3479.1	1828.8	2.27	4	4484.8	2280.9	0	0	3510.2	1691.7	0	0	3498.3	1663.6	0	0	3079.8	1606.7	0	0
		120	3970.3	2121.9	3.31	5	4846.2	2799.9	4.72	4	3766.4	2032.6	4.55	2	4002.9	2182.0	4.48	3	3220.3	1977.3	2.68	2
		Ave/Toa	2977.6	1635.7	2.79	9	3578.7	1950.7	4.72	4	2883.7	1517.0	4.55	2	2954.4	1551.3	4.48	3	2475.7	1444.3	2.68	2
60	40	60	1166.2	1086.4	0	0	861.7	1228.3	0	0	762.6	926.5	0	0	824.9	1001.5	0	0	640.6	871.3	0	0
		80	1550.1	1238.4	0	0	1308.4	1597.0	0	0	1125.4	1038.3	0	0	1180.8	1151.4	0	0	885.0	983.2	0	0
		100	2170.4	1324.6	0	0	1700.8	1838.0	0	0	1215.7	1339.4	0	0	1287.5	1420.1	0	0	1092.7	1283.7	0	0
		120	3070.4	1671.9	2.73	4	2061.9	1917.1	0	0	1463.2	1451.1	0	0	1582.8	1504.4	0	0	1373.4	1395.8	0	0
		Ave/Toa	1989.3	1330.3	2.73	4	1483.2	1645.1	0	0	1141.7	1188.8	0	0	1219.0	1269.4	0	0	997.9	1133.5	0	0
	50	60	1882.2	1231.9	0	0	1394.7	1047.3	0	0	968.9	846.6	0	0	1109.5	890.5	0	0	877.5	791.4	0	0
		80	3051.0	1671.8	2.55	5	2507.9	1439.9	0	0	2219.1	1117.1	0	0	2169.4	1113.7	0	0	1893.7	1057.6	0	0
		100	4377.9	2374.8	5.42	9	2808.9	1968.6	0	0	2350.2	1468.0	0	0	2576.6	1527.3	0	0	2033.9	1413.3	0	0
		120	–	–	–	19	4475.1	2176.6	5.46	4	3289.9	1747.1	5.47	4	3319.0	1752.9	5.27	5	3162.0	1692.1	3.74	4
		Ave/Toa	3103.7	1759.5	3.99	33	2796.7	1658.1	5.46	4	2207.0	1294.7	5.47	4	2293.6	1321.1	5.27	5	1991.8	1238.6	3.74	4
	60	60	2469.4	1475.3	0	0	2003.3	1267.9	0	0	1588.9	1088.9	0	0	1565.9	1144.4	0	0	1322.5	1033.8	0	0
		80	3980.0	2196.1	4.55	9	3734.5	1847.2	3.33	8	3305.4	1648.0	2.46	5	3399.8	1607.9	2.31	5	2907.4	1551.9	2.52	2
		100	5137.0	2807.0	7.57	11	4885.7	2478.0	4.56	8	4010.1	1887.6	4.58	9	4098.9	1860.1	4.55	9	3680.3	1803.5	3.1	3
		120	–	–	–	20	5346.3	2996.3	7.28	13	4366.3	2228.8	6.77	12	4503.4	2378.7	6.72	12	3820.4	2173.9	4.88	6
		Ave/Toa	3862.1	2159.5	6.06	40	3992.5	2147.4	5.06	29	3317.7	1713.3	4.6	26	3392.0	1747.8	4.53	26	2932.7	1640.8	3.5	11

Table 5. Comparison results between integrated and sequential approaches.

Instance			Integrated			Sequential			
$\|I\|$	$\|J_n\|$	$\|G\|$	ATC	AEFC	ARSFC	ATC	AEFC	ARSFC	CI (%)
50	40	60	1.29	0.82	0.47	1.45	0.79	0.66	13.06
		80	1.79	1.05	0.74	1.97	1.03	0.94	9.80
		100	2.59	1.44	1.15	2.66	1.41	1.25	2.92
		120	3.14	1.70	1.43	3.40	1.74	1.66	8.29
	50	60	1.57	0.87	0.70	1.73	0.84	0.89	10.35
		80	2.10	1.26	0.84	2.40	1.27	1.13	14.29
		100	2.87	1.64	1.23	3.14	1.58	1.56	9.42
		120	3.95	2.19	1.77	4.14	2.10	2.04	4.75
	60	60	1.99	1.17	0.82	2.25	1.20	1.06	13.27
		80	2.77	1.59	1.17	3.00	1.53	1.47	8.38
		100	3.57	2.04	1.53	3.72	2.03	1.69	4.13
		120	4.67	2.64	2.03	4.85	2.59	2.25	3.74
	Ave		2.69	1.53	1.16	2.89	1.51	1.38	8.53

Note: The cost data needs to be multiplied by 10^7. Ave denotes the average value of each metric for all instances.

then solve the *DRM* with the resulting values of variables y_{jt}, z_{jkt}, h_{jkt}, and Δ_{kt} being fixed.

We use the instances with $|I| = 50, |J_n| \in \{40, 50, 60\}$, and $|G| \in \{60, 80, 100, 120\}$ to perform the comparison experiments. For the solution obtained from each solution approach, we report the average total cost (ATC), average evacuation flow cost (AEFC), average relief supplies flow cost (ARSFC), and the total cost increase in percentage (CI (%)), which is calculated as $(ATC(Sequential) - ATC(Integrated)) \times 100/ATC(Integrated)$. The comparation results are depicted in Table 5.

From Table 5, as expected, we can observe that our integrated fashion can yield significant total cost savings over the sequential solution approach. This is because the integrated solution approach aims at finding the global optimal solution, whereas the sequential solution approach gives priority to the evacuation planning problem to minimise the evacuation flow cost. Indeed, when comparing the solutions obtained from the sequential solution approach with those from the integrated solution approach, the evacuation flow cost decreases by 1.31% on average, whereas the relief supplies flow cost increases by 18.97% on average, leading to a total cost increase of 8.53% on average. This result clearly demonstrates that it is beneficial to employ the integrated solution approach to solve the DRHND-FLRIAEP.

5.5. Sensitivity analysis

In this section, we discuss the impacts of some model parameters on the solution structure using the instances with $|I| = 60$, $|J_n| = 60$, $|G| = 60$ and $|T| = 2$.

In order to measure the impacts on the solution structure caused by changing parameters, we use the following metrics: (i) the average total cost (ATC); (ii) the average proportion of the number of un-evacuated people (APUEP), measuring the rescue efficiency; (iii) the average total relief supplies stored in distribution centres (ATRS); and (iv) the average total relief supplies transported to rescue shelters (ATRT).

5.5.1. Impacts of uncertainty set parameters $\mathcal{G}$ and ϵ_1

We first analyse the influence of uncertainty set parameters $\mathcal{G}$ and ϵ_1 in the distributionally ambiguity set Φ_κ. Figures 3 and 4 depict how ATC, APUEP, ATRS and ATRT change with the variations of $g \in \{0.5, 1.0, 1.5, 2.0, 2.5\}$ and $\epsilon_1 \in \{0.05, 0.10, 0.15, 0.20, 0.25\}$, respectively.

From Figure 3(a), we can find that ATC decreases with g, but APUEP increases when increasing g. To be precise, the rate of increase in APUEP becomes sharp with the increase of g, implying that a larger g has a stronger impact on the number of un-evacuated people. This is expected since with the increase of g, the uncertainty of supply demands represented by the ambiguity set decreases, which results in the decrease of the average total cost and makes the resulting first-stage solution less robust and flexible, so more injured people fail to evacuate in out-of-sample test. Figure 3(b) depicts that both ATRS and ATRT decrease with g increases. This is because when the uncertainty decreases, the decision maker can obtain more information, so there is no need to transport and store too much relief supplies to yield more conservative solutions.

Figure 4(a) shows that when increasing ϵ_1 related to the evacuation rate of injured people, ATC increases but APUEP decreases, both of which vary in an almost linear way. That is because when ϵ_1 increases, ATRT and ATRS increase, resulting in an increase in the average total rescue cost and a corresponding decrease in the number of people un-evacuated. As can be seen from Figure 4(b), both ATRT and ATRS increase as the increase of ϵ_1. The reason behind these observations is that increasing ϵ_1 will increase the number of injured people that should be evacuated, which results in the decrease of the number of people un-evacuated, and increase the storage and transporting costs of relief supplies.

5.5.2. Impacts of parameter γ_{rt}

We now let $\gamma_{rt} = \gamma$ and discuss the impact of γ by varying the value of $\gamma \in \{0.1, 0.2, 0.3, \ldots, 0.8, 0.9\}$.

From Figure 5(a,b), we can easily find that there is a threshold ($\gamma = 0.5$), before which ATC, APUEP, ATRS and ATRT all slightly change. When γ exceeds the threshold 0.5, ATC, ATRS and ATRT significantly decrease, whereas APUEP sharply increases with increasing γ. The possible reason is that the total amount of relief supplies can only meet part of the realised

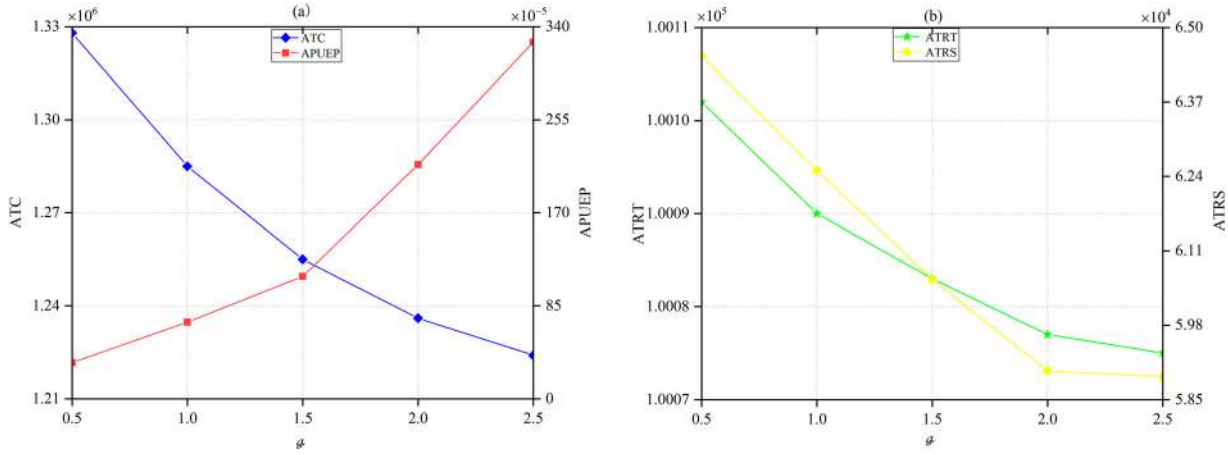

Figure 3. Impacts of uncertainty parameter $\mathcal{G}$.

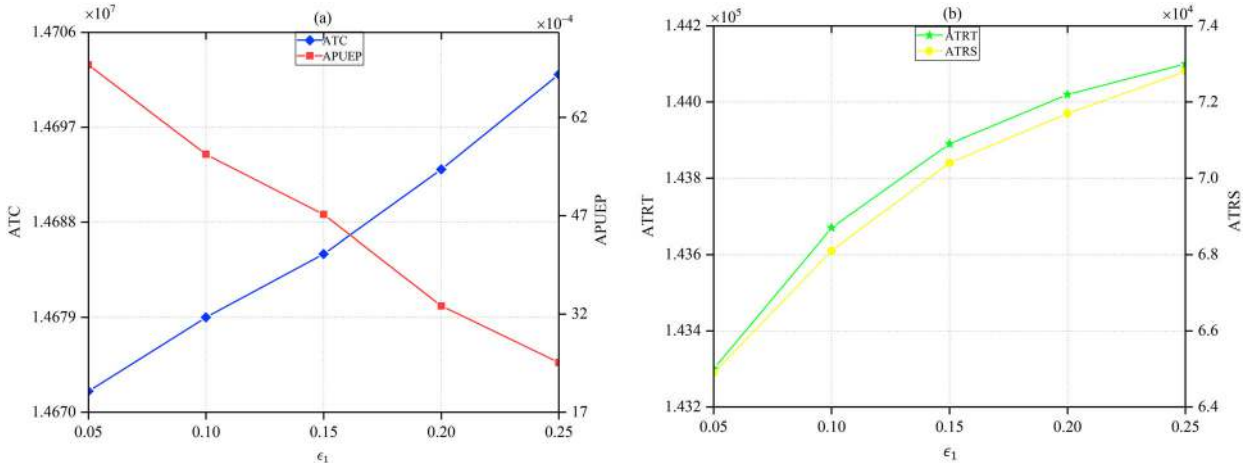

Figure 4. Impacts of uncertainty parameter ϵ_1.

demands for the injured people under the current setting. It follows that there is a threshold ($\gamma = 0.5$) for the risk level γ, below which the number of injured people whose demands can be met relatively stable, implying that varying $\gamma \in \{0.1, 0.2, 0.3, 0.4, 0.5\}$ will not dramatically affect the optimal solution. On the other hand, with high risk level ($\gamma > 0.5$), the relief supplies can potentially meet the demands for more injured people. In this case, it is more beneficial to transfer more injured people from affected areas to rescue shelters as the increase of γ, so the proportion of the number of un-evacuated people dramatically decreases. Moreover, the solution space becomes larger with a larger γ, which increases the chance to find a better solution, so the total cost decreases.

5.5.3. Impacts of parameters ω and ∂

In this subsection, we analyse the impact of the inventory capacity Q_{ir} of relief supplies and unit penalty cost of non-evacuees τ by varying the parameters $\omega \in \{0.1, 0.2, 0.3, 0.4, 0.5\}$ and $\partial \in \{0.3, 0.4, 0.5, 0.6, 0.7\}$.

We first discuss the impact of the inventory capacity of relief supplies on ATC, APUEP, ATRS and ATRS. As shown in Figure 6, with the increasing of parameter ω, ATC, APUEP and ATRS all increase, whereas ATRT decreases. Specifically, the increasing trends of ATC, APUEP and ATRS with ω are analogous, the rate of increase in each metric firstly increase sharply, and eventually even moved beyond a threshold ($\omega = 0.3$). On the other hand, the rate of decrease in ATRT firstly decreases sharply up to a certain threshold 0.3, and then remains constant. The possible reason behind these observations may be that when increasing ω, the inventory capacity of relief supplies at each emergency relief distribution centre decreases, resulting in the decrease of the total supply amount of relief supplies. This further leads to a dramatic increase in the number of people un-evacuated, and an increase of initial stock level.

Figure 7 illustrates how the unit penalty parameter ∂ affects ATC, APUEP, ATRS and ATRT. Because increasing ∂ will increase the penalty cost per un-evacuated person in each time period, the results in Figure 7(a,b) show

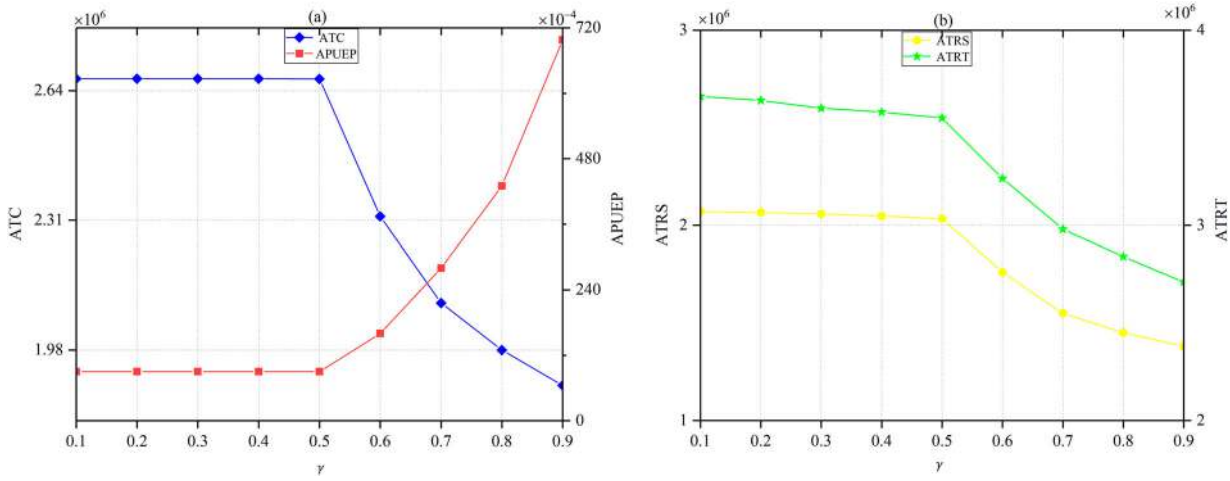

Figure 5. Impacts of parameter γ.

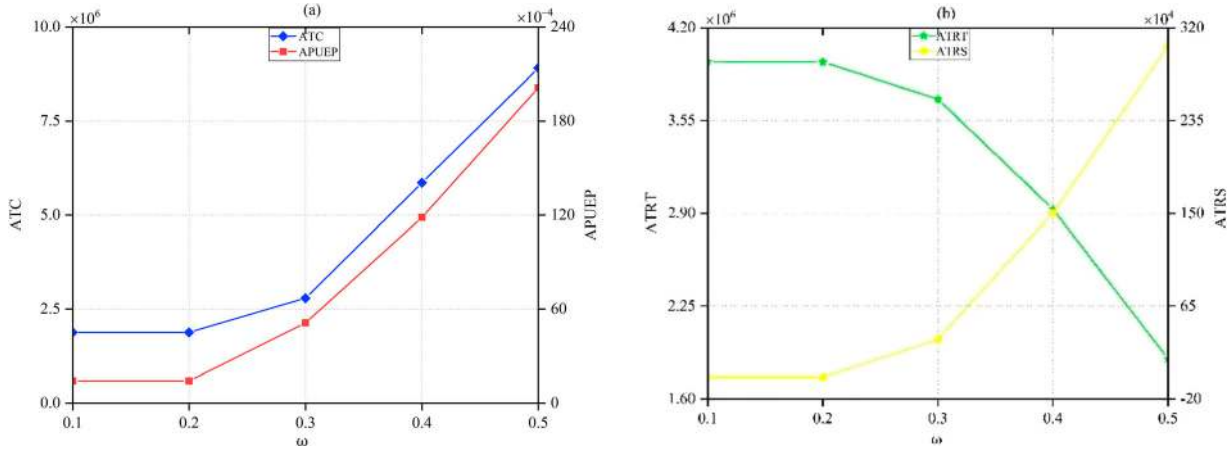

Figure 6. Impacts of parameter ω.

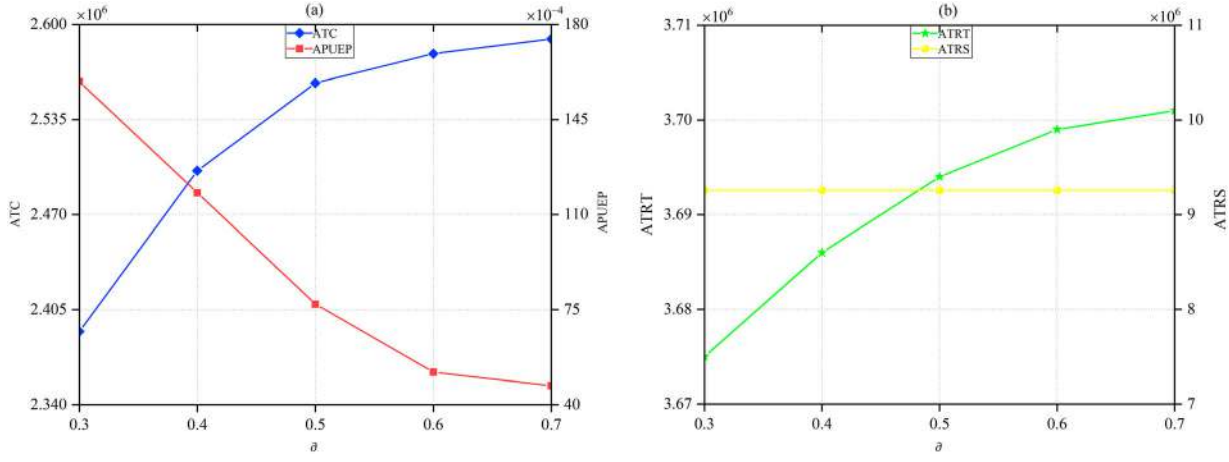

Figure 7. Impacts of parameter ∂.

that, as expected, both ATC and ATRT increase, whereas APUEP decreases and ATRS remains unchanged when increasing ∂. What is more, we also find that the increasing trend of ATC and ATRT and the decreasing trend of APUEP tapers off, which indicate that the influence of ∂ on ATC, ATRT and APUEP gradually decreases.

Overall, the above observations show that all the considered parameters have significant impact on the considered metrics, which informs the decision maker how to set proper parameters so as to achieve the desired trade-off among the considered metrics.

6. Conclusion

In this paper, we develop a distributionally robust model for the integrated facility location, supply inventory and allocation, and evacuation planning problem with multiple types of relief supplies under uncertain demands with only limited distributional information being available and uncertain evacuation rates of injured people. Considering the intractability of the distributionally robust model, we employ the strong duality theory to transform it into a tractable mixed integer linear programme, and adapt the branch-and-Benders-cut algorithm to solve the resulting model into optimality. To improve the performance of the developed algorithm, we introduce two algorithm enhancements, i.e. in–out Benders cut generation and initial cut generation. The experimental results show that the introduced algorithm enhancements can greatly reduce the CPU time, and that the distributionally robust model can provide more robust and flexible solutions in uncertain environments compared with the *SM* and *DM*. The results also show that using a sequential solution approach yields a total cost increase of 8.53% on average instead of our integrated solution approach for the instances with $|I| = 50$, which highlights the benefit of using an integrated solution approach to solve the DRHND-FLRIAEP. Moreover, our analysis of the impacts of the key model parameters further informs the decision makers of how to respond to situational changes on the spot by properly changing the parameter settings.

In the future, researchers can continue to explore from the following perspectives. First, the model involves the allocation of relief supplies, but does not consider the transportation time, which is one of the major factors that affect rescue efficiency. Thus, it is interesting to integrate routing decisions of delivery vehicles alone or delivery vehicles and drones in a collaborative way into the model. Second, we assume that all the injured people are in the same status that require identical relief supplies. However, in real disaster relief, the affected people may be partitioned several types, such as lightly injured persons, severely injured persons, etc., according to the extent of the injury. It is worth considering affected people with different kinds of injuries and investigating corresponding solution structures. Third, we only employ first-order moment information to construct ambiguity set. Another interesting future direction is to use second-order moment information or statistical distance-based ambiguity sets or scenario-based ambiguity sets to measure the uncertainty of demands. Fourth, we only consider the allocation and evacuation operations in the designed humanitarian relief network. To achieve an efficient rescue, it is of interest to consider subcontracting strategy (Dolgui and Proth 2011; Dolgui and Proth 2013), where part of relief supplies demands can be met by the distribution centres on the outside of the network, or some injured people can be transferred to the rescue shelters on the outside of the network. Finally, we assume that the uncertain demands and evacuation rates of injured people are independent, but they may be correlated in some real practice. Thus, it is interesting to consider different ambiguity sets with some correlations between uncertain demands and evacuation rates of injured people, and analyse their corresponding solution structures.

Disclosure statement

No potential conflict of interest was reported by the author(s).

Notes on contributors

Yunqiang Yin received the Ph.D. degree from Beijing Normal University, Beijing, China, in 2009. He is currently a Professor in the School of Management and Economics, University of Electronic Science and Technology of China, Chengdu. His research interests are in production and operations management, medical operations management, and machine learning. He has published more than 80 papers in various international journals including *Transportation Research: Part B, Naval Research Logistics*, *Omega*, *European Journal of Operational Research*, *International Journal of Production Research*, *IEEE Transactions on Industrial Informatics*, *IEEE Transactions on Cybernetics*, *IEEE Transactions on SMC*, *IEEE T-ITS*, etc.

Jie Wang received a master's degree from Sichuan Normal University in 2020. He is currently pursuing a PhD in management science and engineering at UESTC. His research interests include humanitarian relief network design, facility location-allocation and vehicle routing.

Feng Chu is currently a Distinguished Professor of Operations Research at the University of Evry and University of Paris Saclay, France and the head of the AROBAS (Algorithmic, Operations Research, Bioinformatics and Statistical learning) group of the IBISC laboratory. She is the author/co-author of more than 140 papers in scientific journals. She is awarded by the French ministry of Education for her Doctoral Supervision and Research Activities (PEDR) since 2005 and an expert of the European Science Foundation (ESF) and the French Ministry of Higher Education, Research and Innovation (CIR). Her research interests include operations research, stochastic optimisation and their applications in complex systems, such as intelligent transportation systems and logistics and production

systems. Dr. Chu served as an Associate Editor for the IEEE T-SMC, Part C from 2010 to 2013. She is currently an Associate Editor for IJPR, IEEE T-ITS and IEEE T-ASE.

Dujuan Wang received the B.S. and M.S. degrees in Computer Science and Technology, and the Ph.D. degree in Management Science and Engineering from the Dalian University of Technology (DUT), Dalian, China. She is currently a professor in Business School, Sichuan University, Chengdu, China. Her research interests are in logistics and supply chain management, service operation management and optimisation, and machine learning. She has published more than 80 papers in various international journals including *Transportation Research Part B, Naval Research Logistics*, *Omega*, *European Journal of Operational Research*, *IEEE Transactions on SMC*, *International Journal of Production Economics, Computers & Operations Research, Knowledge-Based Systems*, etc. Prof. Wang is currently an Assistant Editor-in-Chief for the *Modern Supply Chain Research and Applications Journal*, and an Associate Editor for *Complex and Intelligent Systems Journal*.

Data availability statement

Data available on request from the authors.

Funding

This paper was supported in part by the National Natural Science Foundation of China under grant numbers 71971041, 72171161 and 71871148 and by the Major Program of National Social Science Foundation of China under grant number 20&ZD084.

References

Alizadeh, M., M. Amiri-Aref, N. Mustafee, and S. Matilal. 2019. "A Robust Stochastic Casualty Collection Points Location Problem." *European Journal of Operational Research* 279 (3): 965–983. https://doi.org/10.1016/j.ejor.2019.06.018

Avishan, F., M. Elyasi, I. Yanikoglu, A. Ekici, and O. O. Ozener. 2023. "Humanitarian Relief Distribution Problem: An Adjustable Robust Optimization Approach." *Transportation Science*, https://doi.org/10.1287/trsc.2023.1204.

Bayram, V., and H. Yaman. 2018. "Shelter Location and Evacuation Route Assignment Under Uncertainty: A Benders Decomposition Approach." *Transportation Science* 52 (2): 416–436. https://doi.org/10.1287/trsc.2017.0762

Ben-Ameur, W., and J. Neto. 2007. "Acceleration of Cutting-Plane and Column Generation Algorithms: Applications to Network Design." *Networks* 49 (1): 3–17. https://doi.org/10.1002/net.20137

Ben-Tal, A., B. Do Chung, S. R. Mandala, and T. Yao. 2011. "Robust Optimization for Emergency Logistics Planning: Risk Mitigation in Humanitarian Relief Supply Chains." *Transportation Research Part B-Methodological* 45 (8): 1177–1189. https://doi.org/10.1016/j.trb.2010.09.002

Caunhye, A. M., and X. Nie. 2018. "A Stochastic Programming Model for Casualty Response Planning During Catastrophic Health Events." *Transportation Science* 52 (2): 437–453. https://doi.org/10.1287/trsc.2017.0777

Caunhye, A. M., Y. Zhang, M. Li, and X. Nie. 2016. "A Location-Routing Model for Prepositioning and Distributing Emergency Supplies." *Transportation Research Part E-Logistics and Transportation Review* 90: 161–176. https://doi.org/10.1016/j.tre.2015.10.011

Dalal, J., and H. Üster. 2018. "Combining Worst Case and Average Case Considerations in an Integrated Emergency Response Network Design Problem." *Transportation Science* 52 (1): 171–188. https://doi.org/10.1287/trsc.2016.0725

Dalal, J., and H. Üster. 2021. "Robust Emergency Relief Supply Planning for Foreseen Disasters Under Evacuation-Side Uncertainty." *Transportation Science* 55 (3): 553–813. https://doi.org/10.1287/trsc.2020.1020

Das, R., and S. Hanaoka. 2014. "Relief Inventory Modelling with Stochastic Lead-Time and Demand." *European Journal of Operational Research* 235 (3): 616–623. https://doi.org/10.1016/j.ejor.2013.12.042

Dolgui, A., and J. M. Proth. 2011. *Supply Chain Engineering: Useful Methods and Techniques*. New York: Springer.

Dolgui, A., and J. M. Proth. 2013. "Outsourcing: Definitions and Analysis." *International Journal of Production Research* 51 (23–24): 6769–6777. https://doi.org/10.1080/00207543.2013.855338

Dyen, A., N. Aras, and Barbarosolu Gülay. 2012. "A Two-Echelon Stochastic Facility Location Model for Humanitarian Relief Logistics." *Optimization Letters* 6 (6): 1123–1145. https://doi.org/10.1007/s11590-011-0421-0

Fischetti, M., I. Ljubic, and M. Sinnl. 2016. "Redesigning Benders Decomposition for Large-Scale Facility Location." *Management Science* 63 (7): 2049–2395. https://doi.org/10.1287/mnsc.2016.2461.

Hu, S., C. Han, Z. S. Dong, and L. Meng. 2019. "A Multi-Stage Stochastic Programming Model for Relief Distribution Considering the State of Road Network." *Transportation Research Part B-Methodological* 123: 64–87. https://doi.org/10.1016/j.trb.2019.03.014

Li, Y., and S. H. Chung. 2019. "Disaster Relief Routing Under Uncertainty: A Robust Optimization Approach." *IISE Transactions* 51 (8): 869–886. https://doi.org/10.1080/24725854.2018.1450540

Li, Y., G. Yu, and J. Zhang. 2021. "A Three-Stage Stochastic Model for Emergency Relief Planning Considering Secondary Disasters." *Engineering Optimization* 53 (4): 551–575. https://doi.org/10.1080/0305215X.2020.1740920

Li, Y., J. Zhang, and G. Yu. 2020. "A Scenario-Based Hybrid Robust and Stochastic Approach for Joint Planning of Relief Logistics and Casualty Distribution Considering Secondary Disasters." *Transportation Research Part E-Logistics and Transportation Review* 141: 102029. https://doi.org/10.1016/j.tre.2020.102029

Liu, K. L., Q. F. Li, and Z. H. Zhang. 2019. "Distributionally Robust Optimization of an Emergency Medical Service Station Location and Sizing Problem with Joint Chance Constraints." *Transportation Research Part B-Methodological* 119: 79–101. https://doi.org/10.1016/j.trb.2018.11.012

Luo, Z., Y. Yin, D. Wang, T. C. E. Cheng, and C. C. Wu. 2023. "Wasserstein Distributionally Robust Chance-Constrained Program with Moment Information." *Computers & Operations Research* 152: 106150. https://doi.org/10.1016/j.cor.2023.106150

Magnanti, T. L., and R. T. Wong. 1981. "Accelerating Benders Decomposition: Algorithmic Enhancement and Model Selection Criteria." *Operations Research* 29 (3): 464–484. https://doi.org/10.1287/opre.29.3.464

Mete, H. O., and Z. B. Zabinsky. 2010. "Stochastic Optimization of Medical Supply Location and Distribution in Disaster Management." *International Journal of Production Economics* 126 (1): 76–84. https://doi.org/10.1016/j.ijpe.2009.10.004

Mohammadi, S., S. A. Darestani, B. Vahdani, and A. Alinezhad. 2020. "A Robust Neutrosophic Fuzzy-Based Approach to Integrate Reliable Facility Location and Routing Decisions for Disaster Relief Under Fairness and Aftershocks Concerns." *Computers & Industrial Engineering* 148: 106734. https://doi.org/10.1016/j.cie.2020.106734

Ni, W., J. Shu, and M. Song. 2018. "Location and Emergency Inventory Pre-Positioning for Disaster Response Operations: Min-Max Robust Model and a Case Study of Yushu Earthquake." *Production and Operations Management* 27 (1): 160–183. https://doi.org/10.1111/poms.12789

Papadakos, N. 2008. "Practical Enhancements to the Magnanti–Wong Method." *Operations Research Letters* 36 (4): 444–449. https://doi.org/10.1016/j.orl.2008.01.005

Rahimian, H., G. Bayraksan, and M. T. Homem-de. 2019. "Identifying Effective Scenarios in Distributionally Robust Stochastic Programs with Total Variation Distance." *Mathematical Programming* 173 (1-2): 393–430. https://doi.org/10.1007/s10107-017-1224-6

Salmerón, J., and A. Apte. 2010. "Stochastic Optimization for Natural Disaster Asset Prepositioning." *Production and Operations Management* 9 (5): 561–574. https://doi.org/10.1111/j.1937-5956.2009.01119.x

Setiawan, E., J. Liu, and A. French. 2019. "Resource Location for Relief Distribution and Victim Evacuation After a Sudden-Onset Disaster." *IISE Transactions* 51 (8): 830–846. https://doi.org/10.1080/24725854.2018.1517284

Shehadeh, K. S., and E. L. Tucker. 2022. "Stochastic Optimization Models for Location and Inventory Prepositioning of Disaster Relief Supplies." *Transportation Research Part C-Emerging Technologies* 144: 103871. https://doi.org/10.1016/j.trc.2022.103871

Üster, H., and J. Dalal. 2017. "Strategic Emergency Preparedness Network Design Integrating Supply and Demand Sides in a Multi-Objective Approach." *IISE Transactions* 49 (4): 395–413. https://doi.org/10.1080/0740817X.2016.1234731

Wang, S., Z. Chen, and T. Liu. 2020. "Distributionally Robust hub Location." *Transportation Science* 54 (5): 1153–1438. https://doi.org/10.1287/trsc.2019.0941

Wang, D., K. Yang, and L. Yang. 2023. "Risk-averse two-Stage Distributionally Robust Optimization for Logistics Planning in Disaster Relief Management." *International Journal of Production Research* 61 (2): 668–691. https://doi.org/10.1080/00207543.2021.2013559

Yang, M., Y. Liu, and G. Yang. 2021. "Multi-period Dynamic Distributionally Robust pre-Positioning of Emergency Supplies Under Demand Uncertainty." *Applied Mathematical Modelling* 89: 1433–1458. https://doi.org/10.1016/j.apm.2020.08.035

Yang, Y., Y. Yin, D. Wang, I. Joshua, T. C. E. Cheng, and L. Dhamotharan. 2023. "Distributionally Robust Multi-Period Location-Allocation with Multiple Resources and Capacity Levels in Humanitarian Logistics." *European Journal of Operational Research* 305 (3): 1042–1062. https://doi.org/10.1016/j.ejor.2022.06.047

Yin, Y., Z. Luo, D. Wang, and T. C. E. Cheng. 2023. "Wasserstein Distance-Based Distributionally Robust Parallel-Machine Scheduling." *Omega* 120: 102896. https://doi.org/10.1016/j.omega.2023.102896

Zhang, P., Y. Liu, G. Yang, and G. Zhang. 2022. "A Multi-Objective Distributionally Robust Model for Sustainable Last Mile Relief Network Design Problem." *Annals of Operations Research* 309 (2): 689–730. https://doi.org/10.1007/s10479-020-03813-3

Zhang, J., H. Liu, G. Yu, J. Ruan, and F. Chan. 2019. "A Three-Stage and Multi-Objective Stochastic Programming Model to Improve the Sustainable Rescue Ability by Considering Secondary Disasters in Emergency Logistics." *Computers & Industrial Engineering* 135: 1145–1154. https://doi.org/10.1016/j.cie.2019.02.003

Zhang, J., Y. Liu, G. Yu, and Z.-J. Shen. 2021. "Robustifying Humanitarian Relief Systems Against Travel Time Uncertainty." *Naval Research Logistics* 68 (7): 871–885. https://doi.org/10.1002/nav.21981

Zhu, L., Y. Gong, Y. Xu, and J. Gu. 2019. "Emergency Relief Routing Models for Injured Victims Considering Equity and Priority." *Annals of Operations Research* 283 (1-2): 1573–1606. https://doi.org/10.1007/s10479-018-3089-3

Zymler, S., D. Kuhn, and B. Rustem. 2013. "Distributionally Robust Joint Chance Constraints with Second-Order Moment Information." *Mathematical Programming* 137 (1-2): 167–198. https://doi.org/10.1007/s10107-011-0494-7

Appendices

1. The proof of proposition 3.4

Given any $r \in R, t \in \{1, 2, \cdots, T\}$, define the worst-case conditional value-at-risk (CVaR) at level $1-\gamma_{rt}$ of random variable $\tilde{\kappa}_{rt}$ under distribution $\mathbb{P} \in \mathbb{F}_\kappa$ as the random variable governed by $\mathbb{P}$ as follows:

$$\begin{aligned}\sup_{\in_\kappa} -\mathrm{CVaR}_{\gamma_{rt}}\left(\tilde{\kappa}_{rt}\sum_{j\in N\cup E}\sum_{k\in G}h_{jkt}n_{kt}-\sum_{i\in M}\sum_{j\in N\cup E}q_{ijrt}\right)\\ =\inf_{\beta\in}\left\{\beta+\frac{1}{\gamma_{rt}}\sup\left(\left[\tilde{\kappa}_{rt}\sum_{j\in N\cup E}\sum_{k\in G}h_{jkt}n_{kt}\right.\right.\right.\\ \left.\left.\left.-\sum_{i\in M}\sum_{j\in N\cup E}q_{ijrt}-\beta\right]^+\right)\right\}.\end{aligned}$$

By Theorem 2.2 in Zymler, Kuhn, and Rustem (2013), the distributionally robust chance constraint

$$\inf_{\in_\kappa}\left\{\sum_{i\in M}\sum_{j\in N\cup E}q_{ijrt}\geq\tilde{\kappa}_{rt}\sum_{j\in N\cup E}\sum_{k\in G}h_{jkt}n_{kt}\right\}\geq 1-\gamma_{rt}$$

is equal to:

$$\sup_{\in_\kappa} -\mathrm{CVaR}_{\gamma_{rt}}\left(\tilde{\kappa}_{rt}\sum_{j\in N\cup E}\sum_{k\in G}h_{jkt}n_{kt}-\sum_{i\in M}\sum_{j\in N\cup E}q_{ijrt}\right)\leq 0 \tag{A1}$$

$$\Leftrightarrow \inf_{\beta\in}\left\{\beta+\frac{1}{\gamma_{rt}}\sup\left(\left[\tilde{\kappa}_{rt}\sum_{j\in N\cup E}\sum_{k\in G}h_{jkt}n_{kt}-\sum_{i\in M}\sum_{j\in N\cup E}q_{ijrt}-\beta\right]^{+}\right)\right\}\leq 0 \tag{A2}$$

The inner term $\sup\left(\left[\tilde{\kappa}_{rt}\sum_{j\in N\cup E}\sum_{k\in G}h_{jkt}n_{kt}-\sum_{i\in M}\sum_{j\in N\cup E}q_{ijrt}-\beta\right]^{+}\right)$ can be reformulated as the following optimisation problem:

$$\sup\int_{\boldsymbol{\kappa}\in Q}\left[\tilde{\kappa}_{rt}\sum_{j\in N\cup E}\sum_{k\in G}h_{jkt}n_{kt}-\sum_{i\in M}\sum_{j\in N\cup E}q_{ijrt}-\beta\right]^{+}d \tag{A3}$$

s.t.

$$\int_{\boldsymbol{\kappa}\in Q}\tilde{\kappa}_{rt}d=\mu_{rt} \tag{A4}$$

$$\int_{\boldsymbol{\kappa}\in Q}(\tilde{\kappa}_{rt}-\mu_{rt})d\leq\sigma_{rt} \tag{A5}$$

$$\int_{\boldsymbol{\kappa}\in Q}-(\tilde{\kappa}_{rt}-\mu_{rt})d\leq\sigma_{rt} \tag{A6}$$

$$\int_{\boldsymbol{\kappa}\in Q}\sum_{l=1}^{t}1'(\tilde{\boldsymbol{\kappa}}^{l}-\boldsymbol{\mu}^{l})d\leq\xi_{t} \tag{A7}$$

$$\int_{\boldsymbol{\kappa}\in Q}-\sum_{l=1}^{t}1'(\tilde{\boldsymbol{\kappa}}^{l}-\boldsymbol{\mu}^{l})d\leq\xi_{t} \tag{A8}$$

$$\int_{\boldsymbol{\kappa}\in Q}d_{r}=1 \tag{A9}$$

Let $\eta_{rt},\phi_{rt}^{+},\phi_{rt}^{-},\Gamma_{t}^{+},\Gamma_{t}^{-}$ and θ be the Lagrange multipliers associated with the constraints (36)–(41), respectively. By the strong duality theory, we can obtain the dual result of above optimisation problem as follows:

$$\min\mu_{rt}\eta_{rt}+\sigma_{rt}(\phi_{rt}^{+}+\phi_{rt}^{-})+\xi_{t}(\Gamma_{t}^{+}+\Gamma_{t}^{-})+\theta \tag{A10}$$

s.t.

$$\begin{aligned}&\tilde{\kappa}_{rt}\eta_{rt}+(\tilde{\kappa}_{rt}-\mu_{rt})(\phi_{rt}^{+}-\phi_{rt}^{-})\\&\quad+\sum_{l=1}^{t}\sum_{\boldsymbol{r}'\in R}(\tilde{\kappa}_{r'l}-\mu_{r'l})(\Gamma_{t}^{+}-\Gamma_{t}^{-})+\theta\\&\geq\tilde{\kappa}_{rt}\sum_{j\in N\cup E}\sum_{k\in G}h_{jkt}n_{kt}-\sum_{i\in M}\sum_{j\in N\cup E}q_{ijrt}-\beta,\\&\quad\forall\boldsymbol{r}'\in R,\tilde{\kappa}_{r't}\in[l_{r't},e_{r't}]\end{aligned} \tag{A11}$$

$$\begin{aligned}&\tilde{\kappa}_{rt}\eta_{rt}+(\tilde{\kappa}_{rt}-\mu_{rt})(\phi_{rt}^{+}-\phi_{rt}^{-})\\&\quad+\sum_{l=1}^{t}\sum_{\boldsymbol{r}'\in R}(\tilde{\kappa}_{r'l}-\mu_{r'l})(\Gamma_{t}^{+}-\Gamma_{t}^{-})+\theta\geq 0,\\&\quad\forall\boldsymbol{r}'\in R,\tilde{\kappa}_{rt}\in[l_{rt},e_{rt}]\end{aligned} \tag{A12}$$

$$\phi_{rt}^{+},\phi_{rt}^{t-},\Gamma_{t}^{+},\Gamma_{t}^{-}\geq 0 \tag{A13}$$

Let $A_{rt}=\left|\eta_{rt}+\phi_{rt}^{+}-\phi_{rt}^{-}+\Gamma_{t}^{+}-\Gamma_{t}^{-}-\sum_{j\in N\cup E}\sum_{k\in G}h_{jkt}n_{kt}\right|$, $B_{rt}=|\eta_{rt}+\phi_{rt}^{+}-\phi_{rt}^{-}+\Gamma_{t}^{+}-\Gamma_{t}^{-}|$ and $C^{t}=|\Gamma_{t}^{+}-\Gamma_{t}^{-}|$. By Lemma 3.3, constraints (43) and (44) can be equivalently reformulated as follows:

$$\begin{aligned}&\kappa_{rt}^{*}\left(\eta_{rt}+\phi_{rt}^{+}-\phi_{rt}^{-}+\Gamma_{t}^{+}-\Gamma_{t}^{-}-\sum_{j\in N\cup E}\sum_{k\in G}h_{jkt}n_{kt}\right)\\&\quad-\zeta_{rt}A_{rt}+\sum_{t'=1}^{t}\sum_{\boldsymbol{r}'\in R,(r',t')\neq(r,t)}(\kappa_{r't'}^{*}(\Gamma_{t}^{+}-\Gamma_{t}^{-})-\zeta_{r't'}C_{t})\\&\quad-\mu_{rt}(\phi_{rt}^{+}-\phi_{rt}^{-})-\sum_{t'=1}^{t}\sum_{\boldsymbol{r}'\in R}\mu_{r't'}(\Gamma_{t}^{+}-\Gamma_{t}^{-})+\theta\\&\geq-\sum_{i\in M}\sum_{j\in N\cup E}q_{ijrt}-\beta\end{aligned} \tag{A14}$$

$$\begin{aligned}&\kappa_{rt}^{*}(\eta_{rt}+\phi_{rt}^{+}-\phi_{rt}^{-}+\Gamma_{t}^{+}-\Gamma_{t}^{-})-\zeta_{rt}B_{rt}\\&\quad+\sum_{t'=1}^{t}\sum_{\boldsymbol{r}'\in R,(r',t')\neq(r,t)}(\kappa_{r't'}^{*}(\Gamma_{t}^{+}-\Gamma_{t}^{-})-\zeta_{r't'}C_{t})\\&\quad-\mu_{rt}(\phi_{rt}^{+}-\phi_{rt}^{-})-\sum_{t'=1}^{t}\sum_{\boldsymbol{r}'\in R}\mu_{r't'}(\Gamma_{t}^{+}-\Gamma_{t}^{-})+\theta\geq 0\end{aligned} \tag{A15}$$

$$\eta_{rt}+\phi_{rt}^{+}-\phi_{rt}^{-}+\Gamma_{t}^{+}-\Gamma_{t}^{-}-\sum_{j\in N\cup E}\sum_{k\in G}h_{jkt}n_{kt}\geq-A_{rt} \tag{A16}$$

$$\eta_{rt}+\phi_{rt}^{+}-\phi_{rt}^{-}+\Gamma_{t}^{+}-\Gamma_{t}^{-}-\sum_{j\in N\cup E}\sum_{k\in G}h_{jkt}n_{kt}\leq A_{rt} \tag{A17}$$

$$\eta_{rt}+\phi_{rt}^{+}-\phi_{rt}^{-}+\Gamma_{t}^{+}-\Gamma_{t}^{-}\geq-B_{rt} \tag{A18}$$

$$\eta_{rt}+\phi_{rt}^{+}-\phi_{rt}^{-}+\Gamma_{t}^{+}-\Gamma_{t}^{-}\leq B_{rt} \tag{A19}$$

$$\Gamma_{t}^{+}-\Gamma_{t}^{-}\geq-C_{t} \tag{A20}$$

$$\Gamma_{t}^{+}-\Gamma_{t}^{-}\leq C_{t} \tag{A21}$$

$$A_{rt},B_{rt},C_{t}\geq 0 \tag{A22}$$

Substituting the model consisting of the objective function (A10), constraints (A13) and (A14)–(A22) into constraints (A2), the result follows.

2. The pseudo-code of the basic benders decomposition algorithm

Algorithm 1

Set l=0, $UB = +\infty$, $LB = -\infty$, and $EP = ER = \emptyset$

While $UB \neq LB$ do:

  Solve the current relaxed MP and obtain $(\overline{\mathbf{x}}, \overline{\mathbf{y}}, \overline{\mathbf{z}}, \overline{D})$

  $LB \leftarrow \sum_{t=1}^{T}\sum_{i\in M} f_{it}^{d}\overline{x}_{it} + \sum_{t=1}^{T}\sum_{j\in N} f_{jt}^{r}\overline{y}_{jt} + \overline{D}$

  Solve DS $(\overline{\mathbf{x}}, \overline{\mathbf{y}}, \overline{\mathbf{z}})$ to obtain $(\boldsymbol{p},\ \boldsymbol{l}^{+}, \boldsymbol{l}^{-}, \boldsymbol{f},\ \boldsymbol{e}, \boldsymbol{g}, \boldsymbol{v}^{+}, \boldsymbol{v}^{-}, \boldsymbol{s}, \boldsymbol{\rho}, \boldsymbol{u}^{+},\ \boldsymbol{o}^{+},\ \boldsymbol{w}^{+},\ \boldsymbol{w}^{-}, \boldsymbol{\Upsilon}^{+}, \boldsymbol{\Upsilon}^{-})$ and z_{DS}^{l}

  If z_{DS}^{l} is bounded, then

    $UB \leftarrow \max\{UB, \sum_{t=1}^{T}\sum_{i\in M} f_{it}^{d}\overline{x}_{it} + \sum_{t=1}^{T}\sum_{j\in N} f_{jt}^{r}\overline{y}_{jt} + z_{DS}^{l}\}$

    Add $(\boldsymbol{p},\ \boldsymbol{l}^{+}, \boldsymbol{l}^{-}, \boldsymbol{f},\ \boldsymbol{e}, \boldsymbol{g}, \boldsymbol{v}^{+}, \boldsymbol{v}^{-}, \boldsymbol{s}, \boldsymbol{\rho}, \boldsymbol{u}^{+},\ \boldsymbol{o}^{+},\ \boldsymbol{w}^{+},\ \boldsymbol{w}^{-}, \boldsymbol{\Upsilon}^{+}, \boldsymbol{\Upsilon}^{-})$ to EP

  Else

    Add $(\boldsymbol{p},\ \boldsymbol{l}^{+}, \boldsymbol{l}^{-}, \boldsymbol{f},\ \boldsymbol{e}, \boldsymbol{g}, \boldsymbol{v}^{+}, \boldsymbol{v}^{-}, \boldsymbol{s}, \boldsymbol{\rho}, \boldsymbol{u}^{+},\ \boldsymbol{o}^{+},\ \boldsymbol{w}^{+},\ \boldsymbol{w}^{-}, \boldsymbol{\Upsilon}^{+}, \boldsymbol{\Upsilon}^{-})$ to ER

  $l \leftarrow l + 1$

3. Stochastic model by SAA method

Based on the selected training samples $\tilde{\boldsymbol{\kappa}}^{l}, l \in L$, we formulate the SM as follows:

$$\min \sum_{t=1}^{T}\sum_{i\in M} f_{it}^{d}x_{it} + \sum_{t=1}^{T}\sum_{j\in N} f_{jt}^{r}y_{jt} + \frac{1}{|L|}\sum_{l\in L}\sum_{t=1}^{T}\sum_{i\in M}\sum_{j\in N\cup E}\sum_{r\in R} c_{ijt}^{t}q_{ijrt}^{l} + \sum_{t=1}^{T}\sum_{i\in M}\sum_{r\in R} c_{irt}^{s}\delta_{irt} + \sum_{t=1}^{T}\sum_{k\in G}\sum_{j\in N\cup E} Len_{jk}c_{jkt}^{e}h_{jkt}n_{kt} + \sum_{t=1}^{T}\sum_{k\in G}\tau_{kt}\Delta_{kt}n_{kt}$$

Subject to

Constraint (4)–(5), (8), (11)–(17), (19)

$$\sum_{i\in M} q_{ijrt}^{l} \leq y_{jt}Q_{j}^{ri} \quad \forall j \in N, r \in R, t \in \{1, 2, \cdots T\}, l \in L \tag{A23}$$

$$\sum_{i\in M} q_{ijrt}^{l} \leq Q_{j}^{ri} \quad \forall j \in E, r \in R, t \in \{1, 2, \cdots T\}, l \in L \tag{A24}$$

$$\sum_{j\in N\cup E} q_{ijrt}^{l} \leq x_{it}Q_{ir}^{d} \quad \forall i \in M, r \in R, t \in \{1, 2, \cdots T\}, l \in L \tag{A25}$$

$$\delta_{irt} = \delta_{ir,t-1} + \vartheta_{irt} - \sum_{j\in N\cup E} q_{ijrt}^{l} \quad \forall i \in M, r \in R, t \in \{1, 2, \cdots T\}, l \in L \tag{A26}$$

$$\tilde{\kappa}_{rt}^{l}\sum_{j\in N\cup E}\sum_{k\in G} h_{jkt}n_{kt} - \sum_{i\in M}\sum_{j\in N\cup E} q_{ijrt}^{l} \leq M_{big}a_{rt}^{l} \quad \forall r \in R, t \in \{1, 2, \cdots T\}, l \in L \tag{A27}$$

$$\sum_{l\in L}(1 - a_{rt}^{l}) \leq |L|(1 - \gamma_{rt}) \quad \forall r \in R, t \in \{1, 2, \cdots T\} \tag{A28}$$

$$a_{rt}^{l} \in \{0, 1\}, d_{ijrt}^{l} \geq 0, \quad \forall i \in M, j \in N \cup E, r \in R, k \in G, t \in T, l \in L \tag{A29}$$

Here q_{ijrt}^{l} denotes the amount of relief supplies r transported from emergency relief distribution centre i to rescue shelter j during period t in scenario l, and a_{rt}^{l} is a binary variable equal to 1 if and only if the amount of relief supplies r is satisfied with the demand of injured people in scenario l, and M_{big} is a big constant. Constraints (A23) and (A24) together state that relief supplies can only be delivered to the usable rescue shelters, and that the amount of relief supplies delivered to a rescue shelter should not exceed its maximum inventory capacity in scenario l; Constraint sets means that the amount of relief supplies delivered from the opened emergency relief distribution centre in each time period cannot exceed its maximum inventory capacity in scenario l; Constraints (A26) give the distribution and storage balance equation at each emergency relief distribution centre in each time period in scenario l; Constraints (A27) and (A28) are the linearisation of the distributionally robust chance constraints; Constraints (A27) determine a_{rt}^{l}; Constraints (A28) ensure the probability tolerance; and Constraints (A29) define the decision variables.

4. The performance of different φ

By varying the parameter $\varphi \in \{0.3, 0.5, 0.7, 0.9, 0.99, 1\}$„ we can derive the different performance of the proposed branch-and-Benders-cut algorithm. Table A1 shows how average CPU time varies by varying the parameter $\varphi \in \{0.3, 0.5, 0.7, 0.9, 0.99, 1\}$. The results clearly demonstrate that $\varphi = 0.9$ is superior to the other φ values in most cases. Thus, we set $\varphi = 0.9$ in the subsequent experiments.

Table A1. Performance of different φ.

Instances ($\|I\|$, $\|J_n\|$, $\|G\|$)			Average CPU time					
			$\varphi = 0.3$	$\varphi = 0.5$	$\varphi = 0.7$	$\varphi = 0.9$	$\varphi = 0.99$	$\varphi = 1$
40	40	60	695.3	892.1	822.5	**322.4**	331.6	387.2
		80	1380.3	1336.0	1126.5	**572.6**	613.0	696.5
		100	2170.3	1951.2	1976.4	**603.3**	743.1	817.8
		120	2908.6	2558.5	2266.4	**1034.2**	1146.3	1262.6
	50	60	995.3	978.2	1004.3	447.4	**437.2**	501.8
		80	1415.7	1373.2	1404.1	**601.5**	865.6	1238.2
		100	2892.2	2931.9	2606.7	**1125.3**	1577.5	1826.6
		120	3743.4	3795.7	3503.7	**1440.5**	2049.4	2890.8
	60	60	1893.5	1228.2	1525.7	**847.6**	887.4	986.1
		80	2208.9	1840.1	1890.0	**1495.8**	1497.1	1614.4
		100	2559.4	2801.5	3191.2	**2116.9**	2255.3	2496.2
		120	5045.8	5344.3	4744.2	**3058.8**	3119.6	3433.7
50	40	60	961.8	920.1	872.0	**430.1**	513.6	543.9
		80	1433.0	1411.2	1496.2	**604.7**	665.0	758.8
		100	2239.3	2300.6	2373.0	**722.3**	841.2	898.6
		120	3544.3	3070.5	2915.2	**1246.4**	1326.7	1472.1
	50	60	1438.8	1459.7	1499.4	**726.4**	790.0	856.8
		80	2084.6	2036.7	2138.0	**1282.1**	1333.1	1446.9
		100	3579.5	3440.6	3297.2	**1516.1**	2247.7	2381.0
		120	4579.1	4445.5	4296.7	**2517.7**	3157.4	2975.5
	60	60	2178.9	2231.2	2003.4	**1147.0**	1188.1	1232.2
		80	3691.0	3621.4	3553.6	**2966.3**	2990.4	3091.5
		100	3766.6	3720.5	3688.5	**3387.7**	3454.7	3585.8
		120	3855.0	4055.2	3791.9	**3684.7**	3748.2	3943.7
60	40	60	1286.8	1092.1	1182.6	1179.1	**669.0**	777.5
		80	2175.4	2196.6	1803.8	**1107.4**	1192.1	1511.6
		100	2745.3	2698.6	2825.0	**917.7**	1167.0	1326.4
		120	4129.4	4033.1	3928.8	**1384.1**	1586.3	1878.8
	50	60	1740.3	1862.2	1983.9	**809.4**	997.5	1075.8
		80	3301.1	3443.5	3196.8	**1441.7**	2216.3	2371.4
		100	4712.5	4936.3	5285.9	**2018.1**	2398.1	2599.0
		120	5349.6	4901.8	4870.7	**2935.5**	3291.5	3373.4
	60	60	2633.8	2827.6	2798.0	**1510.9**	1599.5	1649.3
		80	3735.5	4066.5	4255.0	**3245.8**	3308.2	3661.2
		100	4408.6	4661.4	4771.9	**3956.5**	3983.3	4179.1
		120	5581.9	5601.7	5374.3	**4254.1**	4359.3	4348.2

Note: Bold value indicates the minimum CPU time.